Cell Reports
Medicine

Article

siRNA-AGO2 complex inhibits bacterial gene translation: A promising therapeutic strategy for superbug infection

Graphical abstract

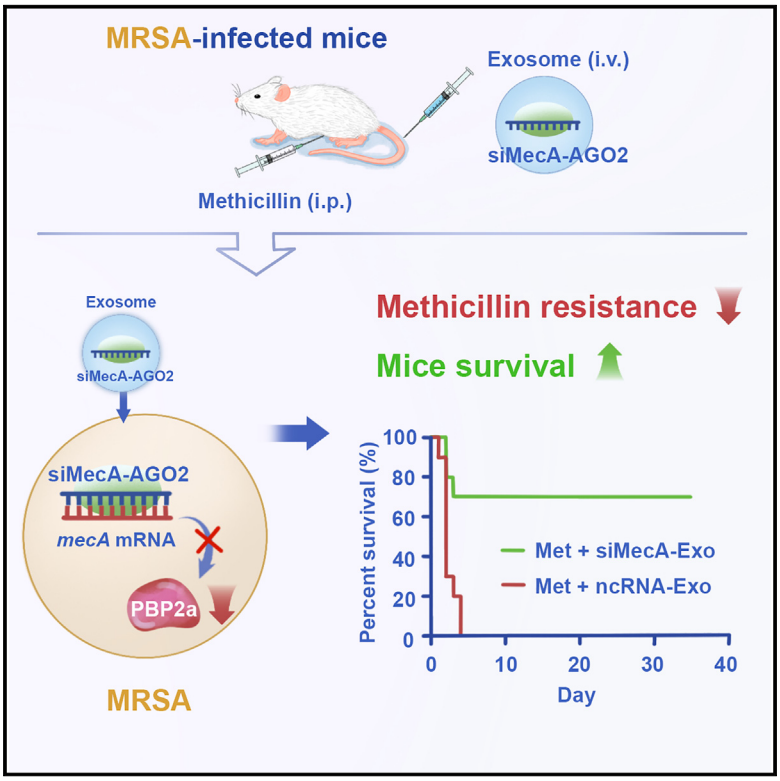

Highlights

- Exosomal siRNA-AGO2 complex can be delivered into bacteria
- Exosomal siRNA inhibits bacterial gene translation in an AGO2-dependent manner
- Exosomal siMecA resensitizes MRSA to methicillin by silencing the *mecA* gene
- *In vivo* self-assembled siMecA-Exos improve the efficacy of methicillin in mice

Authors

Chen Wang, Wangjian Sheng, Yu Zhou, ..., Chen-Yu Zhang, Hongkai Bi, Huan Wang

Correspondence

lingh@ems.hrbmu.edu.cn (H.L.), cyzhang@nju.edu.cn (C.-Y.Z.), hkbi@njmu.edu.cn (H.B.), wanghuan@nju.edu.cn (H.W.)

In brief

Wang et al. report that the exosomal siRNA-AGO2 complex silences the target bacterial gene by translational repression without mRNA degradation and consequently develop a therapeutic strategy to improve the efficacy of antibiotics against superbacterial infection, which uses *in vivo* self-assembled siRNA to silence the antibiotic resistance gene.

Wang et al., 2025, Cell Reports Medicine *6*, 101997
March 18, 2025 © 2025 The Authors. Published by Elsevier Inc.
https://doi.org/10.1016/j.xcrm.2025.101997

CellPress

Cell Reports Medicine

CellPress
OPEN ACCESS

Article

siRNA-AGO2 complex inhibits bacterial gene translation: A promising therapeutic strategy for superbug infection

Chen Wang,[1,2,8] Wangjian Sheng,[3,8] Yu Zhou,[1,8] Xudong Hang,[4,8] Jiayi Zhao,[1,8] Yuanyuan Gu,[1] Xiangfeng Meng,[1] Yuefan Bai,[5] Weili Li,[1] Yujing Zhang,[1] Linlin Zhang,[6] Jing Yu,[1] Zhen Zhou,[1] Xiaona Li,[1] Haorui Sun,[1] Yanhong Xue,[7] Tao Xu,[7] Ke Zen,[1] Hong Ling,[6,*] Chen-Yu Zhang,[1,*] Hongkai Bi,[4,5,*] and Huan Wang[3,9,*]

[1]Nanjing Drum Tower Hospital Center of Molecular Diagnostic and Therapy, Research Unit of Extracellular RNA, Chinese Academy of Medical Sciences, State Key Laboratory of Pharmaceutical Biotechnology, Jiangsu Engineering Research Center for MicroRNA Biology and Biotechnology, NJU Advanced Institute of Life Sciences (NAILS), NJU Institute of Artificial Intelligence Biomedicine and Biotechnology, School of Life Sciences, Nanjing University, Nanjing, Jiangsu 210023, China

[2]School of Pharmacy, Jiangsu University, Zhenjiang, Jiangsu 212013, China

[3]State Key Laboratory of Coordination Chemistry, Jiangsu Key Laboratory of Advanced Organic Materials, School of Chemistry and Chemical Engineering, Nanjing University, Nanjing, Jiangsu 210023, China

[4]NHC Key Laboratory of Tropical Disease Control, School of Tropical Medicine, Hainan Medical University, Haikou, Hainan 571199, China

[5]Department of Pathogen Biology, Jiangsu Key Laboratory of Pathogen Biology, Nanjing Medical University, Nanjing, Jiangsu 211166, China

[6]Department of Microbiology, Wu Lien-Teh Institute, Heilongjiang Provincial Key Laboratory of Infection and Immunity, Key Laboratory of Pathogen Biology, Harbin Medical University, Harbin, Heilongjiang 150081, China

[7]National Laboratory of Biomacromolecules, CAS Center for Excellence in Biomacromolecules, Institute of Biophysics, Chinese Academy of Sciences, Beijing 100101, China

[8]These authors contributed equally

[9]Lead contact

*Correspondence: lingh@ems.hrbmu.edu.cn (H.L.), cyzhang@nju.edu.cn (C.-Y.Z.), hkbi@njmu.edu.cn (H.B.), wanghuan@nju.edu.cn (H.W.)

https://doi.org/10.1016/j.xcrm.2025.101997

SUMMARY

Silencing resistance genes of pathogenic bacteria by RNA interference (RNAi) is a potential strategy to fight antibiotic-resistant bacterial infections. Currently, RNAi cannot be achieved in bacteria due to the lack of RNA-induced silencing complex machinery and the difficulty of small interfering RNA (siRNA) delivery. Here, we show that exosomal siRNAs can be efficiently delivered into bacterial cells and can silence target genes primarily through translational repression without mRNA degradation. The exosomal Argonaute 2 (AGO2) protein forms a complex with siRNAs, which is essential for bacterial gene silencing. Both *in vitro* and *in vivo*-generated exosome-packaged siRNAs resensitize methicillin-resistant *Staphylococcus aureus* (MRSA) to methicillin treatment by silencing the *mecA* gene, which is the primary beta-lactam resistance determinant of MRSA. This approach significantly enhances the therapeutic effect in a mouse model of MRSA infection. In summary, our study provides a method for siRNA delivery to bacteria that may facilitate the treatment of antibiotic-resistant bacterial infection.

INTRODUCTION

Multidrug-resistant bacteria pose a major threat to human health.[1,2] As the introduction of new drugs is significantly slower than the spread of antibiotic resistance, new therapeutic strategies for drug-resistant bacteria are urgently needed. Bacteriophages are promising for the treatment of infections by antibiotic-resistant strains; however, concerns regarding the immune response and phage resistance still need to be addressed.[3] Deleting bacterial virulence genes or antibiotic resistance genes does not put high selective pressure on pathogens, so it is a potential strategy against superbacteria. Advances in CRISPR techniques for gene editing in prokaryotic cells may provide a new opportunity in this regard. However, current bacterial gene-editing efforts are limited to model microorganisms.[4] In addition, the transportation of CRISPR-Cas machinery (e.g., plasmids) into drug-resistant bacteria is generally challenging,[5] and highly efficient *in vivo* delivery systems have not yet been established.

We speculate that the manipulation of bacterial genes at the transcriptional level is a potential strategy to fight antibiotic-resistant bacterial infections by silencing their resistance genes. In eukaryotes, small RNAs (sRNAs) regulate the post-transcriptional gene expression of targets with complementary sequences through RNA interference (RNAi), and a number of sRNA drugs have been used in the clinic.[6–9] However, sRNAs have not been applied to regulate bacterial genes due to the lack of RNAi regulatory machinery, i.e., RNA-induced silencing

This is an open access article under the CC BY-NC license (http://creativecommons.org/licenses/by-nc/4.0/).

complexes (RISCs), in bacteria.[10] In addition, efficient methods for delivering sRNAs to bacteria *in vivo* are not currently available. Extracellular vesicles (EVs) are common secretory vesicles that allow the intercellular exchange of biomolecules in both eukaryotes[11,12] and bacteria.[13] For example, in mammals, circulating microRNAs (miRNAs) are often encapsulated in EVs called exosomes, through which miRNAs are delivered into long-distance recipient cells at low concentrations[14,15]; RISC proteins, including Argonaute 2 (AGO2), a key component of the RNAi machinery that guides the function of secreted miRNAs in mammalian recipient cells,[16] are also packaged in exosomes.[17] Therefore, exosomes hold great potential as delivery vehicles for the transport of sRNAs and RNA regulatory machinery into bacteria.

RESULTS

Exosomes efficiently mediate the delivery of sRNA into *E. coli* cells

To investigate the interaction between exosomes and bacteria, we chose the gram-negative bacterium *Escherichia coli* as a model because it is a common component of the gut microbiota, and some strains are listed as drug-resistant pathogens. To prepare exosomes containing small interfering RNA (siRNA), HEK293T cells were transfected with the synthetic double-stranded RNA (dsRNA) siAda, the guide strand of which is fully complementary to a coding region of the *ada* methyltransferase gene involved in DNA damage repair (Table S1).[18] Exosomes secreted by transfected HEK293T cells, named siAda-Exos, were purified from the culture medium, and the content of siAda guide strand (hereafter called siAda) in siAda-Exos was determined to be 0.3 fmol/(μg exosome) by quantitative reverse-transcription PCR (qRT-PCR) (Figures S1A–S1C). *E. coli* cells were then cocultured with 200 μg/mL siAda-Exos in Luria-Bertani (LB) medium for 6 h before harvesting. The resulting *E. coli* cells were shown to contain 9.0 fmol siAda molecules/10^8 *E. coli* cells (an average of 56 copies per *E. coli* cell) (Figure 1A; Figure S1D). In contrast, no siAda uptake by *E. coli* was detected when an equal amount of free siAda molecules (0.06 nM) was supplied in the LB culture medium. To exclude the possible effect of transfection complexes copurified with exosomes, *E. coli* was cocultured with lipofectamine-loaded siAda instead of siAda-Exos, which resulted in no detectable siAda delivery into *E. coli* (Figure 1A). Thus, the packaging of siAda by exosomes is essential for its delivery into *E. coli*. The uptake of siAda by *E. coli* was most efficient in the logarithmic phase of growth and dependent on the dose of siAda-Exos supplied in the culture medium (Figure S2). Furthermore, the delivery of siAda appears to be more than just a diffusion process, as the final concentration of siAda inside *E. coli* cells (estimated to be ~0.6 nM) was 60-fold higher than that in the culture medium (~0.01 nM) (Figure S1E). To examine whether sRNA transport is dependent on the origins of the exosomes, *E. coli* were cultured with exosomes secreted by various human cell lines, including HEK293T, A549, SW480, TE-10, Caco-2, and SGC-7901 cells. miR-16, an abundant human exosomal miRNA,[19] was detected in all *E. coli* samples (Figure S1F), indicating the generality of sRNA delivery mediated by human cell-derived exosomes. Collectively, our data show that exosomes secreted by human cells can efficiently deliver sRNAs into *E. coli*.

Exosomes deliver sRNAs into the cytoplasm of *E. coli* cells

To investigate the distribution of sRNA after delivery, exosomes containing Cy3-labeled siAda were prepared and cocultured with *E. coli* cells. Cy3 fluorescence was observed in the cytoplasm but not on the membrane of *E. coli* cells, confirming that siAda entered the cells instead of attaching to the bacterial membrane (Figure 1B). When *E. coli* cells were cocultured with exosomes membrane labeled with PKH67, PKH67 fluorescence was detected specifically on the membrane of *E. coli* cells, suggesting that the lipid components of exosomes were integrated with the membrane of *E. coli* (Figure 1C). Immunogold transmission electron microscopy (TEM) analysis indicated that CD63, a human exosomal membrane protein, was found mainly near the membranes of *E. coli* cells treated with exosomes, whereas the AGO2 protein, a key component of the RISC packaged in exosomes,[17] was distributed in the bacterial cytoplasm (Figure 1D). In addition, sRNA profiling identified 26 human exosomal miRNAs in the *E. coli* sample, indicating that both siRNAs and miRNAs were transported into *E. coli* cells (Tables S2 and S3; Figure S1G). A transient interaction between *E. coli* and exosomes revealed by TEM analysis indicated that exosomes adhered to *E. coli* cells at the region where the bacterial cell wall was disintegrated, implying that disintegration of the *E. coli* membrane might be necessary for the uptake of exosomes (Figure S3). This phenomenon is similar to the fusion between *E. coli* cells and the outer membrane vesicles of *P. aeruginosa*.[20] Together, our data indicate that during the uptake of exosomes by *E. coli* cells, internal exosomal components are released into the bacterial cytoplasm, whereas the membrane components of exosomes are integrated with the bacterial membrane.

sRNAs delivered by exosomes silence target genes in *E. coli*

Dose-dependent downregulation of Ada expression was observed in *E. coli* into which siAda was successfully delivered by siAda-Exos compared with samples treated with negative control RNA (ncRNA)-Exos (Figure 2A). ncRNA is a scrambled dsRNA (Table S1), and like siAda, it is processed in mammalian cells into a single guide strand that is loaded into AGO2 and exosomes. We have predicted that ncRNA has no specific target in the genome of *E. coli* or methicillin-resistant *Staphylococcus aureus* (MRSA). The mRNA level of the *ada* gene, however, was not decreased (Figure 2B), suggesting that the silencing of the *ada* gene was primarily caused by translational repression and not mRNA degradation.[21] To provide insights into the mechanism of Ada protein expression downregulation, free siAda was electroporated into *E. coli* cells. Neither *ada* mRNA nor Ada protein expression levels were affected (Figures S4A–S4C), suggesting that the downregulation of Ada protein expression was not a result of siAda-mediated endogenous bacterial RNA regulatory pathways in *E. coli*.[22] We next speculated that gene silencing was facilitated by exosomal components cotransferred into *E. coli*. Immunoprecipitation (IP) analysis indicated that in

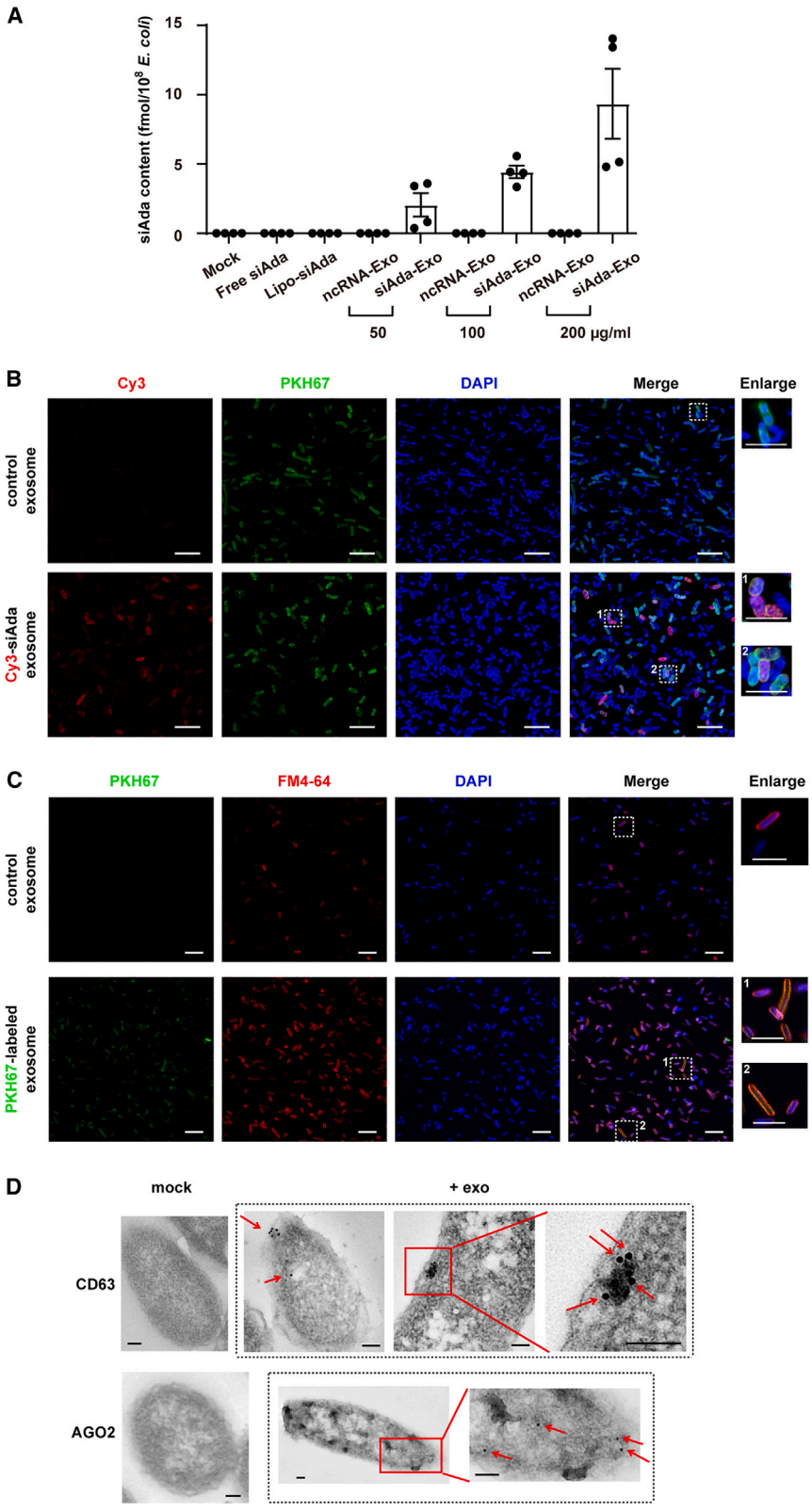

Figure 1. Human exosomes deliver sRNAs into *E. coli*

(A) Dose-dependent delivery of siAda into *E. coli* by exosomes. *E. coli* were cultured with 50, 100, or 200 μg/mL ncRNA-Exo or siAda-Exo, free siAda (0.06 nM), or lipofectamine-incubated siAda (lipo-siAda, 100 fmol/mL) for 6 h. siAda concentrations corresponding to different doses of siAda-Exo were 15, 30, and 60 fmol/mL, respectively. The amount of siAda transferred into *E. coli* was determined by qPCR (n = 4). The data represent mean ± SEM of four biological replicates.

(B) *E. coli* was cultured with exosomes containing Cy3-conjugated siAda (red) or control exosomes. PKH67 (green) was employed to label and show the location of the membrane of *E. coli*. DAPI (blue) was employed to stain DNA in *E. coli* cells. Images were acquired by confocal microscopy. Scale bars, 10 μm (and 5 μm for enlarged images).

(C) *E. coli* was cultured with PKH67-labeled exosomes (green) or control exosomes. The membranes of *E. coli* cells were stained and indicated with FM4-64 (red). Images were acquired by confocal microscopy. Scale bars, 10 μm (and 5 μm for enlarged images).

(D) Representative immuno-TEM images of immunogold labeling of CD63 and AGO2 in *E. coli* incubated with exosomes. Gold particles are depicted as black dots. Scale bars, 100 nm.

See also Figures S1–S3; Tables S2 and S3.

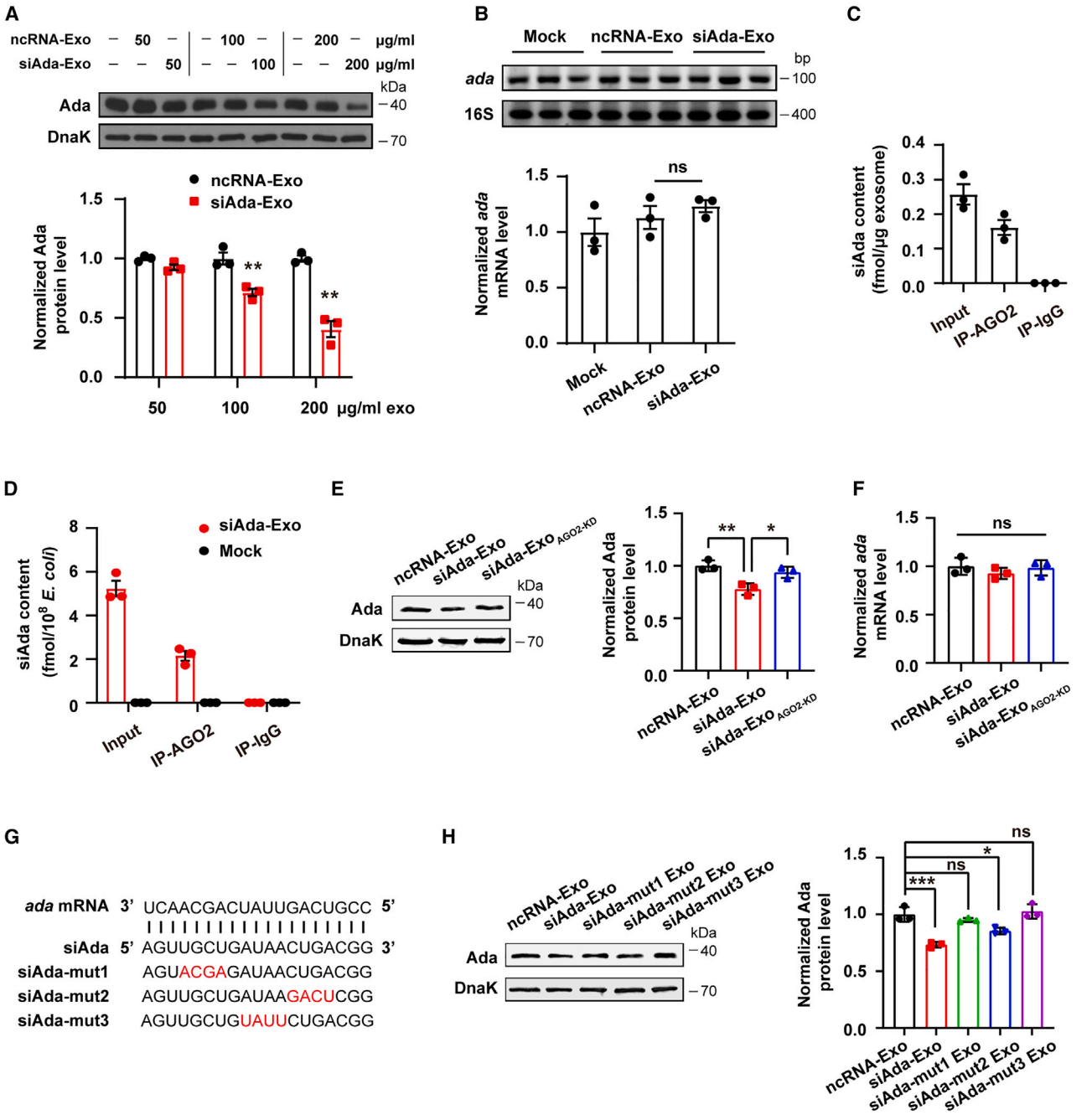

Figure 2. siAda-Exos downregulate the expression of the *ada* gene in *E. coli*

(A) Dose-dependent downregulation of Ada protein expression by siAda-Exos. The expression levels of Ada protein in *E. coli* cultured with ncRNA-Exos or siAda-Exos were determined by western blotting. DnaK was used as a loading control. Lower: quantification of normalized expression levels (n = 3). The asterisks indicate significant differences between ncRNA-Exo and siAda-Exo.

(B) *ada* mRNA expression in *E. coli* cultured with 200 μg/mL ncRNA-Exos or siAda-Exos was quantified by qPCR with 16S rRNA as a reference, and the relative RNA level was determined (bottom, n = 3). Top: *ada* mRNA expression was determined by semiquantitative PCR in triplicate.

(C) IP of the AGO2 protein in siAda-Exos. Total siAda (input) and AGO2-associated siAda (IP-AGO2) levels were determined by qRT-PCR (n = 3). IgG was used as a negative control for IP.

(D) IP of the AGO2 protein in *E. coli* cultured with siAda-Exos. The amount of siAda in the total *E. coli* cell lysate (input) and the AGO2 IP sample (IP-AGO2) was determined by qRT-PCR (n = 3). IP-IgG was used as a negative control.

(E and F) *E. coli* was incubated with 100 μg/mL siAda-Exo (34 fmol/mL of siAda) or 200 μg/mL siAda-Exo$_{AGO2\text{-}KD}$ (38 fmol/mL of siAda). The increased input of siAda-Exo$_{AGO2\text{-}KD}$ aims to achieve equal amount of siAda delivered into *E. coli* as siAda-Exo. The expression levels of Ada protein (E) and *ada* mRNA (F) were quantified by western blotting using DnaK as a loading control, and qPCR with 16S rRNA as a reference, respectively.

(legend continued on next page)

siAda-Exos, the majority of siAda was associated with the AGO2 protein (Figure 2C). These AGO2-siAda complexes were well preserved through the exosome-mediated delivery process and detected in the lysate of *E. coli* cells treated with siAda-Exos (Figure 2D). Studies have shown that human AGO2 bound to a miRNA or an siRNA is sufficient to accurately target and silence target RNAs.[23,24] Therefore, the exosomal AGO2-siAda complex is likely involved in gene silencing in *E. coli* after being delivered into gram-negative bacteria. To investigate the role of AGO2 in siAda-induced gene silencing in *E. coli*, siAda-Exos$_{AGO2\text{-}KD}$ were prepared from AGO2-knockdown HEK293T cells (Figure S5A). The amount of AGO2 in the resulting exosomes was significantly decreased to ~15% of that in the control. The downregulation of Ada protein expression by siAda was reversed by AGO2 knockdown, in spite of the same amount of siAda delivered into *E. coli* (Figures 2E and 2F; Figures S5B and S5C). This indicates that AGO2 is responsible for siAda-mediated gene silencing. To determine whether full complementarity was required for gene regulation in bacteria, we introduced mutations into the siAda sequence in different locations (Figure 2G). The translational repression of the target bacterial gene by exosomal siRNA was still observed when the siRNA sequence was mutated by four nucleotides in the 3′ end, but not in the 5′ end or in the middle (Figure 2H; Figure S6A). The result indicates that exosome-mediated RNAi may function with imperfectly matched sequences. Then, we introduced more mutations into the functional siAda-mut2, but the sequence with additional mismatches lost the gene regulation function (Figures S6B and S6C), which indicated that 4-nt mismatches may be the limit.

Exosome-delivered siMecA reduces the drug resistance of gram-positive MRSA by silencing the *mecA* gene

The gram-positive pathogen MRSA is a frequent cause of fatal infections in humans[25] and contains a chromosomally localized drug-resistant *mecA* gene encoding penicillin-binding protein 2a (PBP2a).[26] We explored whether exosomes can deliver sRNAs targeting the *mecA* gene into MRSA and reduce its antibiotic resistance by downregulating the expression of PBP2a. Exosomes containing siMecA guide strand (hereafter called siMecA, which is fully complementary to a coding region of the *mecA* gene), named siMecA-Exos, were prepared in the same way as siAda-Exos. After coculturing a community-associated (CA)-MRSA USA400 (MW2) strain with 200 μg/mL siMecA-Exo, a concentration of 17.5 fmol siMecA molecules/10^8 MRSA cells (an average of 105 copies per cell) was achieved, and siMecA was successfully delivered into MRSA (Figure 3A; Figure S7A; Table S1). The delivery of siMecA strictly required the packaging of exosomes, as the addition of free siMecA or lipofectamine-incubated siMecA to the culture medium led to no siMecA uptake by MRSA (Figure 3A). Delivery was most efficient during the logarithmic phase of MRSA growth (Figure S8). As expected, the expression of the PBP2a protein in MRSA was significantly decreased in a dose-dependent manner after coculture with siMecA-Exos (Figure 3B; Figure S7B). Again, the mRNA level of the *mecA* gene was not decreased in MRSA treated with siMecA-Exos compared with MRSA samples treated with ncRNA-Exos (Figure 3C), suggesting that gene silencing is primarily caused by translational repression and not mRNA degradation.

We expected the drug resistance of MRSA to be reduced by siMecA-Exo treatment due to a decrease in the level of the PBP2a protein. Indeed, the minimum inhibitory concentration (MIC) of methicillin against three MRSA strains was lowered by 2-fold in the samples treated with siMecA-Exos compared with the samples treated without exosomes or with ncRNA-Exos (Figure 3D). The killing kinetics study demonstrated that methicillin together with siMecA-Exo had stronger bactericidal activity than methicillin alone or together with ncRNA-Exo: a significant reduction in colony-forming units (CFUs) was observed when exposed to siMecA-Exo and methicillin (1× MIC) (Figure 3E).

The AGO2 protein is a key component of the RISC machinery for gene regulation, and AGO2 protein transported via microvesicles is capable of guiding the function of secreted miRNAs in mammalian recipient cells.[16] IP indicated that the majority of siMecA was associated with exosomal AGO2 in siMecA-Exos, and a significant portion of these AGO2-siMecA complexes was delivered into MRSA cells (Figure S7C). Furthermore, AGO2 was found to be associated with *mecA* mRNA, suggesting that siMecA bound to AGO2 might guide the formation of the AGO2-siMecA-(mRNA$_{mecA}$) complex and decrease the expression of the PBP2a protein (Figure 3F). To investigate the role of AGO2 in siMecA-induced gene silencing in MRSA, siMecA-Exos$_{AGO2\text{-}KD}$ were prepared from AGO2-knockdown HEK293T cells (Figure S9A). Upon coculturing of MRSA with siMecA-Exos$_{AGO2\text{-}KD}$, the decrease of PBP2a expression in MRSA and the reduced resistance of MRSA to methicillin by siMecA-Exo were reversed despite the same amount of siMecA input (Figures 3G and 3H), indicating that exosomal AGO2 is essential for siMecA-mediated gene silencing in MRSA. For sRNA-induced translational inhibition to occur in mammalian, zebrafish, and *Drosophila* cells, RISC components other than AGO2, namely, the TNRC6/GW182 proteins, are usually required.[27] The TNRC6/GW182 proteins have been reported to be present in HEK293T-derived exosomes[19] and are likely co-delivered into bacteria to function together with AGO2 to silence bacterial genes. To examine whether GW182 participates in the gene regulation, we prepared siMecA-Exo$_{GW182\text{-}KD}$ from GW182-knockdown HEK293T cells (Figure S9B). The reduction in CFUs by siMecA-Exo was significantly reversed by siMecA-Exo$_{GW182\text{-}KD}$ (Figure 3I), indicating that GW182 contributes to siMecA-mediated gene silencing. In addition, we introduced 3-nt mutations into the siMecA sequence at different positions and prepared corresponding siMecA-mut Exos (Figure 3J; Figure S9C).

(G) Diagram of base-pairing between the target *ada* mRNA and antisense strands of siAda, or siAda mutants (siAda-mut). Mutant nucleotides were marked in red.
(H) *E. coli* was incubated with 200 μg/mL ncRNA-Exo, siAda-Exo, or siAda-mut Exo. The expression levels of Ada protein were determined by western blotting. DnaK was used as a loading control. Right: quantification of normalized expression levels (n = 3).
Data are means ± SEM (A–D) or means ± SD (E–H) of three independent experiments. Statistical significance was determined using two-tailed Student's t test (A and B) and one-way ANOVA with Tukey's multiple hoc test (E, F, and H). *p < 0.05, **p < 0.01, ***p < 0.001. ns, not significant. See also Figures S4–S6.

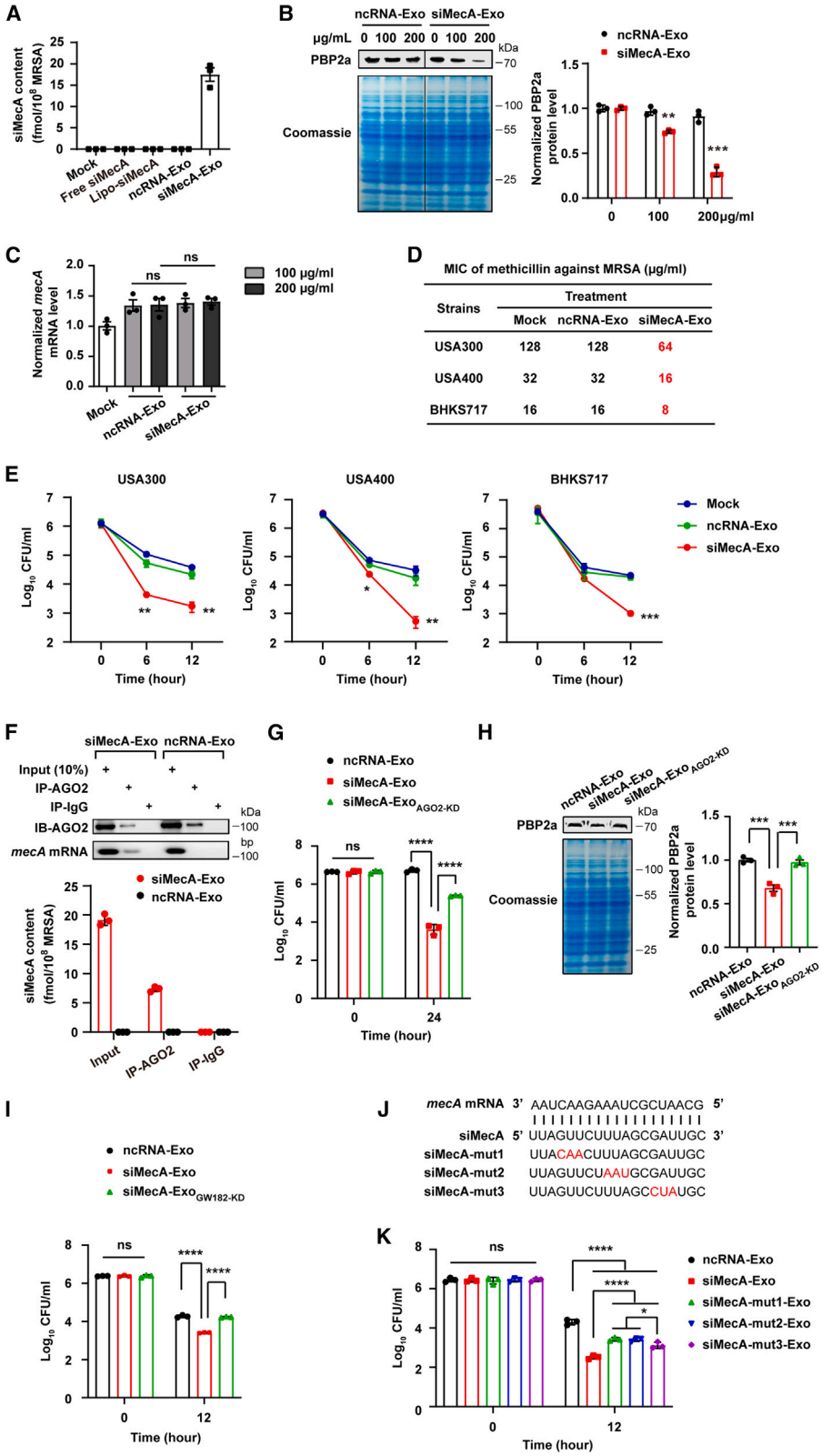

(legend on next page)

Compared with ncRNA-Exo, the three mutants still had strong bactericidal activities in the presence of 1× MIC of methicillin, but they were weaker than siMecA-Exo. Among the three, siMecA-mut3 Exo mutated at the 3′ end was more effective than that mutated at the 5′ end or in the middle (Figure 3K).

To further investigate the mechanism underlying translational repression, we performed an RNA pull-down assay and identified several staphylococcal proteins that may interact with siMecA (Figure S10; Table S4). The major ones were type II NADH:quinone oxidoreductase, succinate-CoA ligase, probable acetyl-CoA acyltransferase, FemB, isocitrate dehydrogenase, RecA, glyceraldehyde-3-phosphate dehydrogenase 2, glucose-6-phosphate isomerase, elongation factor Tu, and pyrimidine nucleoside phosphorylase; among them, elongation factor Tu is most related to translation. Further investigation is needed to identify the key proteins involved in siMecA-mediated gene regulation.

siMecA-Exos improve the efficacy of methicillin in treating MRSA-infected mice

The intriguing exosome-mediated *mecA* gene silencing prompted us to investigate its application in fighting MRSA infections. We speculated that siMecA-Exos would reduce the antibiotic resistance of MRSA *in vivo*, therefore enhancing the therapeutic efficacy of methicillin. To test this hypothesis, BALB/c mice were infected with the CA-MRSA USA400 MW2 strain by intravenous (i.v.) injection and then treated with 3 mg/kg methicillin by intraperitoneal (i.p.) injection and 5 mg/kg siMecA-Exos by tail vein injection (i.v.) every day for 7 consecutive days (Figure 4A). Coadministration of methicillin and siMecA-Exos effectively protected mice from lethal infection (70% survival rate) (Figure 4B, "Met + siMecA-Exo" vs. "Met + ncRNA-Exo": $p = 0.0012$). The mice remained alive during administration and stayed healthy without exhibiting severe side effects for another 28 days. In contrast, administration of methicillin alone failed to reduce mouse mortality, and replacing siMecA with ncRNA in exosomes also abolished their protective effect (Figure 4B, "Met + ncRNA-Exo" vs. "Met": $p = 0.4586$). Accumulation of siMecA was detected in a variety of mouse organs (the liver, spleen, and kidneys) as well as the plasma 24 h after treatment with siMecA-Exos (Figures 4C and 4D). Accordingly, staphylococcal loads were significantly reduced in these organs and the sera of infected mice 24 h after coadministration of methicillin and siMecA-Exos (Figures 4E and 4F, "Met + siMecA-Exo" vs. "Met + ncRNA-Exo": $p = 0.0011$ [serum], 0.0426 [liver], 0.0116 [spleen], and 0.0102 [kidney]). Therefore, the delivery of siMecA by exosomes into MRSA via tail vein injection of siMecA-Exos is not limited to the mouse plasma but also occurs in various organs after exosomes reach them via the circulation. In addition, the levels of inflammatory biomarkers, including tumor necrosis factor alpha and interleukin-6, were significantly decreased, suggesting that coadministration of methicillin and siMecA-Exos relieved MRSA infection (Figure 4G). To further verify the function of siMecA-Exos *in vivo*, we isolated MRSA cells from the blood of infected mice treated with siMecA-Exos and methicillin. Both siMecA and the AGO2 protein were detected in these MRSA cells, and the expression of the PBP2a protein was downregulated (Figures 4H–4J). These results indicate that exosome-mediated delivery of siMecA and silencing of the *mecA* gene indeed occur in mice and directly contribute to the enhanced therapeutic effect of methicillin.

Figure 3. siMecA-Exos downregulate PBP2a expression and sensitize MRSA to methicillin

(A) The amount of siMecA delivered into MRSA by incubation with 200 μg/mL siMecA-Exos for 6 h was determined by qPCR ($n = 3$).

(B) Dose-dependent downregulation of PBP2a protein expression by siMecA-Exos. The expression levels of the PBP2a protein in MRSA incubated with 100 or 200 μg/mL ncRNA-Exos or siMecA-Exos were determined by western blotting. Coomassie staining of total protein is shown and was used to confirm equal loading. Right: quantification of normalized expression levels ($n = 3$). siMecA concentrations corresponding to different doses of siMecA-Exo were 50 and 100 fmol/mL, respectively. The asterisks indicate significant differences between ncRNA-Exo and siMecA-Exo.

(C) The levels of *mecA* mRNA in MRSA incubated with 100 or 200 μg/mL ncRNA-Exos or siMecA-Exos were quantified by qPCR by normalization to the 16S rRNA level ($n = 3$).

(D) Antibacterial activity of methicillin against MRSA strains. By supplementing 100 μg/mL of siMecA-Exo (50 fmol/mL of siMecA) to the culture medium, reduced MIC value of methicillin for MRSA was observed.

(E) The time-dependent killing of MRSA by methicillin (1× MIC) in the presence of 250 μg/mL ncRNA-Exos and siMecA-Exos (150 fmol/mL of siMecA). Data are means ± SD of triplicates. CFUs, colony-forming units. The asterisks indicate significant differences between ncRNA-Exo and siMecA-Exo.

(F) IP of the AGO2 protein in MRSA cultured with siMecA-Exos or ncRNA-Exos. IP efficiency was verified by immunoblotting for AGO2 (IB-AGO2, top), and IgG was used as a negative control. Total siMecA (input) and AGO2-associated siMecA (IP-AGO2) levels in MRSA were determined by qRT-PCR (bottom, $n = 3$). AGO2-associated *mecA* mRNA expression was determined by semiquantitative PCR (middle).

(G) In the presence of methicillin (1× MIC), MRSA was incubated with 200 μg/mL ncRNA-Exos, siMecA-Exos (68 fmol/mL of siMecA), or 300 μg/mL siMecA-Exos$_{AGO2\text{-}KD}$ (64 fmol/mL of siMecA). The increased input of siMecA-Exo$_{AGO2\text{-}KD}$ aims to achieve equal amount of siMecA delivered into MRSA as siMecA-Exo. Viable cells were determined at indicated time points.

(H) MRSA was incubated with 200 μg/mL ncRNA-Exos, siMecA-Exos, or 300 μg/mL siMecA-Exos$_{AGO2\text{-}KD}$. The expression levels of the PBP2a protein in the MRSA samples were determined by western blotting. Coomassie staining of total protein is shown and was used to confirm equal loading. Right: normalized quantification ($n = 3$).

(I) In the presence of methicillin (1×MIC), MRSA was incubated with 200 μg/mL ncRNA-Exo, siMecA-Exo (70 fmol/mL of siMecA), or siMecA-Exo$_{GW182\text{-}KD}$ (85 fmol/mL of siMecA). Viable cells were determined at indicated time points.

(J) Diagram of base-pairing between the target *mecA* mRNA and antisense strands of siMecA, or siMecA mutants (siMecA-mut). Mutant nucleotides were marked in red.

(K) In the presence of methicillin (1×MIC), MRSA was incubated with 250 μg/mL ncRNA-Exos, siMecA-Exos, or siMecA-mut Exos. siMecA concentrations were 100 (siMecA), 75 (siMecA-mut1), 60 (siMecA-mut2), and 150 fmol/mL (siMecA-mut3). Viable cells were determined at indicated time points.

Data are means ± SEM (A–C, F, and H) or means ± SD (E, G, and I–K) of three independent experiments. Statistical significance was determined using two-tailed Student's t test (B and C), one-way ANOVA with Tukey's post hoc test (H), and two-way ANOVA with Tukey's multiple hoc test (E, G, I, and K). $^{*}p < 0.05$, $^{**}p < 0.01$, $^{***}p < 0.001$, $^{****}p < 0.0001$. ns, not significant. See also Figures S7–S10 and S14; Table S4.

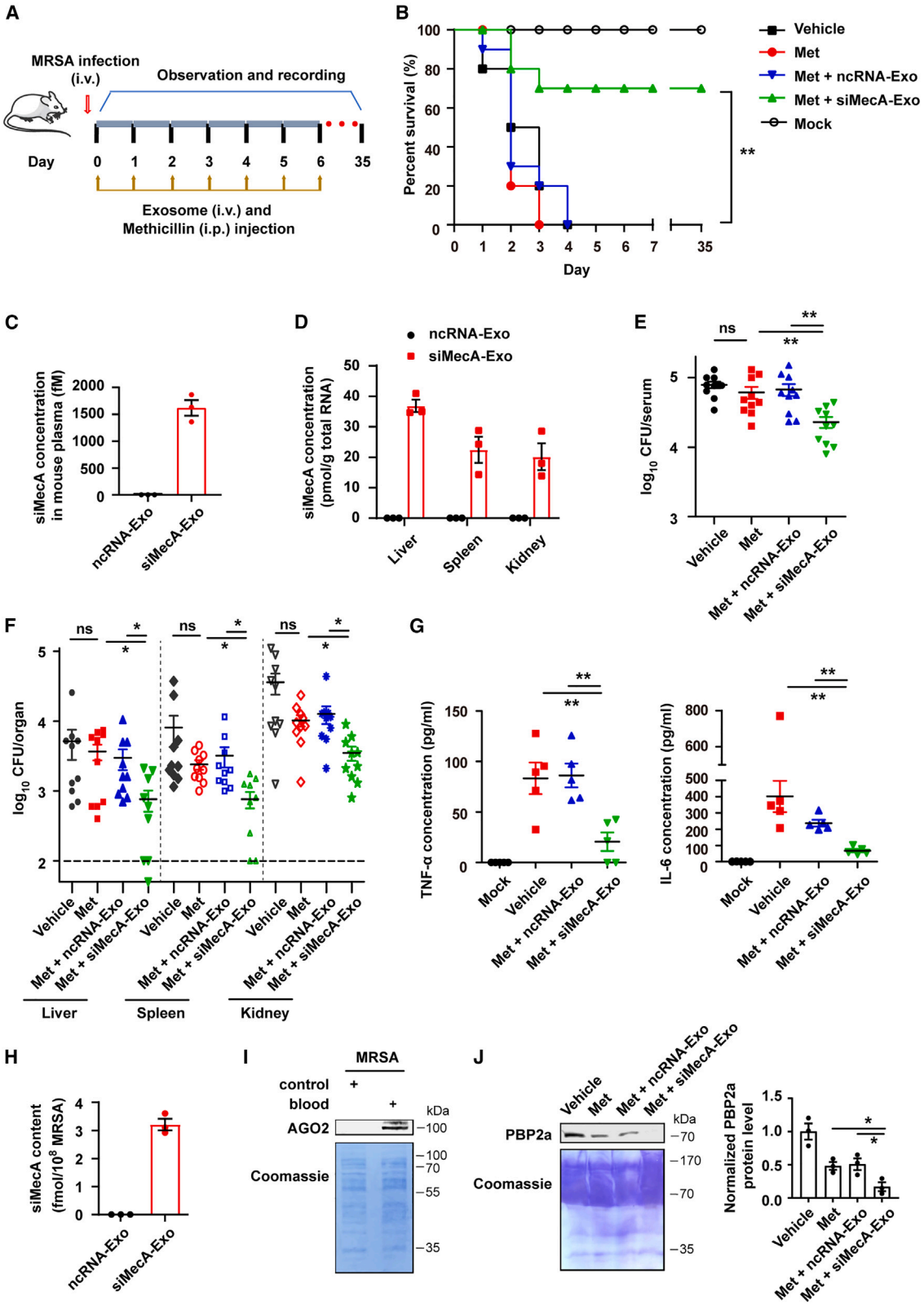

(legend on next page)

CellPress
OPEN ACCESS

In vivo self-assembled siMecA-Exos$_{mice}$ improve the efficacy of methicillin in treating MRSA-infected mice

The utilization of *in vitro*-prepared exosomes for therapeutic purposes is impeded by concerns related to exosome purity, immunogenicity, and carcinogenicity.[28] We recently developed a strategy to reprogram the host liver with genetic circuits to synthesize and secrete exosomes containing specific siRNA sequences into the circulation, which avoids the complications of *in vitro* production and purification procedures and invasive injection.[29] More importantly, since this method utilizes host liver cells to produce secretory exosomes, the issues of immunogenicity and carcinogenicity caused by foreign exosomes are resolved.

Based on this method,[29] we constructed a genetic circuit (siMecA circuit) consisting of two functional modules: the promoter that drives the transcription of siRNA and the siRNA expression cassette that produces the siRNA guide strand (Figure 5A).

Firstly, we tested whether the siMecA circuit has the ability to synthesize functional siMecA *in vitro*. Mouse hepatoma cells (Hepa1-6 cells) were transfected with siMecA circuits. A genetic circuit encoding a scrambled RNA (ncRNA circuit) was used as a negative control. The successful expression and loading of the desired siMecA guide strand into exosomes derived from Hepa1-6 cells (siMecA-Exos$_{mice}$) was verified by qRT-PCR analysis (Figure S11). siMecA-Exos$_{mice}$ were able to deliver siMecA into MRSA and silence the *mecA* gene when cocultured with MRSA *in vitro* (Figure S12).

Next, we examined the *in vivo* production and secretion of siMecA-Exos$_{mice}$ by the mouse liver. The ncRNA circuit or siMecA circuit (5 mg/kg) was intravenously injected into mice, and 9 h later, the amount of siMecA generated in the liver and the amount of siMecA packaged into plasma exosomes were examined, which showed that siMecA-Exos$_{mice}$ were successfully produced and entered the circulation of the mice (Figures 5B and 5C). These results are consistent with the previous findings that the liver can express transgenes introduced by intravenously injected genetic circuits (naked DNA plasmids)[30,31] and can direct the formation of exosome-encapsulated siRNA after taking up the genetic circuits.[29] *In vivo* self-assembled siMecA could reach a concentration of approximately 2,000 fM in the exosome fraction of plasma, which is similar to the previously reported concentration of endogenous exosomal miRNAs that were biologically functional *in vivo*.[32,33]

To evaluate the efficacy of siMecA-Exos$_{mice}$ in facilitating the treatment of MRSA infection by methicillin, the siMecA circuit was injected into mice by tail vein for 7 consecutive days. As expected, coadministration of methicillin and the siMecA circuit effectively protected mice from infection by a lethal dose of MRSA bacteria (Figure 5D, $p < 0.0001$). Ninety percent of mice remained alive until the end of the observation (35 days). Omitting the siMecA circuit or replacing it with an ncRNA circuit failed to reduce mouse mortality. Moreover, staphylococcal loads were significantly reduced in the livers and sera of infected mice 24 h after coadministration of methicillin and the siMecA circuit (Figures 5E and 5F, "Met + siMecA circuit" vs. "Met + ncRNA circuit": $p = 0.0008$ [liver], $p < 0.0001$ [serum]). We used USA300 strain to further test the therapeutic effect of *in vivo* self-assembled siMecA-Exos$_{mice}$ and obtained consistent results. Coadministration of methicillin and the siMecA circuit effectively reduced bacterial loads in the organs and blood (Figures 5G and 5H, $p = 0.0003$ [blood], 0.0004 [liver], 0.0001 [kidney], $p < 0.0001$ [spleen]); moreover, it protected mice from lethal infection (Figure 5I, $p < 0.0001$). These results showed that *in vivo* self-assembled siMecA-Exos$_{mice}$ are effective in silencing the drug resistance gene of MRSA and facilitating antibiotic treatment.

To further confirm the uptake of exosomes by bacteria *in vivo*, we injected a circuit expressing a Lamp2b-GFP fusion protein[29] into MRSA-infected mice by tail vein, to utilize host liver to generate GFP-positive exosomes (Figure S13A). After 24 h, MRSA were isolated from the plasma, and GFP fluorescence was observed on MRSA cells, indicating the *in vivo* uptake of GFP-Exo by MRSA (Figure S13B).

Figure 4. siMecA-Exos enhance the effect of methicillin treatment to protect mice from lethal MRSA infection

(A) Schematic diagram for examining the therapeutic efficacy of siMecA-Exo in a mouse infection model.

(B) Effects of methicillin and siMecA-Exos in protecting mice ($n = 10$) from lethal infection with 5×10^7 CFU of MRSA USA400 MW2. Infected mice received 3 mg/kg methicillin (Met) by intraperitoneal (i.p.) injection and 5 mg/kg siMecA-Exos by tail vein injection (i.v.) every day for 7 days. "Mock" were healthy mice. "Vehicle" were infected mice injected daily (i.p. and i.v.) with PBS. The asterisk indicates a significant difference between ncRNA-Exo and siMecA-Exo.

(C) siMecA levels in the mouse plasma were determined by qRT-PCR ($n = 3$).

(D) siMecA levels in organs (liver, spleen, and kidney) were determined by qRT-PCR ($n = 3$) and normalized to U6 snRNA levels.

(E and F) Effect of methicillin and siMecA-Exos on *S. aureus* survival in the sera (E) and organs (F) ($n = 10$) of mice challenged with USA400 MW2 bacteria 24 h post infection. Each symbol represents the level in 5 μL serum or 10 mg organ sample from an individual mouse. The horizontal bars indicate the mean values, and the dashed lines indicate the limits of detection. The error bars indicate the SEM of the total values.

(G) The inflammation index of mock and infected mice that received different treatments. The levels of TNF-α and IL-6 in the mouse serum were determined by ELISA ($n = 5$). TNF-α, tumor necrosis factor alpha; IL-6, interleukin-6.

(H) MRSA cells were isolated from the plasma of infected mice treated with siMecA-Exos or ncRNA-Exos (10 mice pooled in each group), and RNA was extracted. The resulting siMecA content in MRSA was quantified by qRT-PCR ($n = 3$) and was estimated to be 20 copies per cell.

(I) MRSA cells were isolated from the sera of 10 infected mice, and protein was extracted to determine exosomal AGO2 levels. As a control, *in-vitro*-cultured MRSA was mixed with uninfected blood and subjected to the same procedure as *in vivo* MRSA isolated from the sera of infected mice. Coomassie staining of total protein is shown and was used to confirm equal loading.

(J) PBP2a protein expression levels in MRSA isolated from the sera of infected mice administered various treatments (10 mice pooled in each group), as determined by western blotting. An equal number of MRSA cells were loaded, and Coomassie staining of total protein was used to confirm equal loading. Right: quantification of normalized expression ($n = 3$).

All data are means ± SEM. n = number of biological replicates. Statistical significance was determined using log rank test (B), one-way ANOVA with Tukey's or Dunnett's post hoc test (E and F), Mann-Whitney test (G), and two-tailed Student's t test (J). $^*p < 0.05$, $^{**}p < 0.01$. ns, not significant.

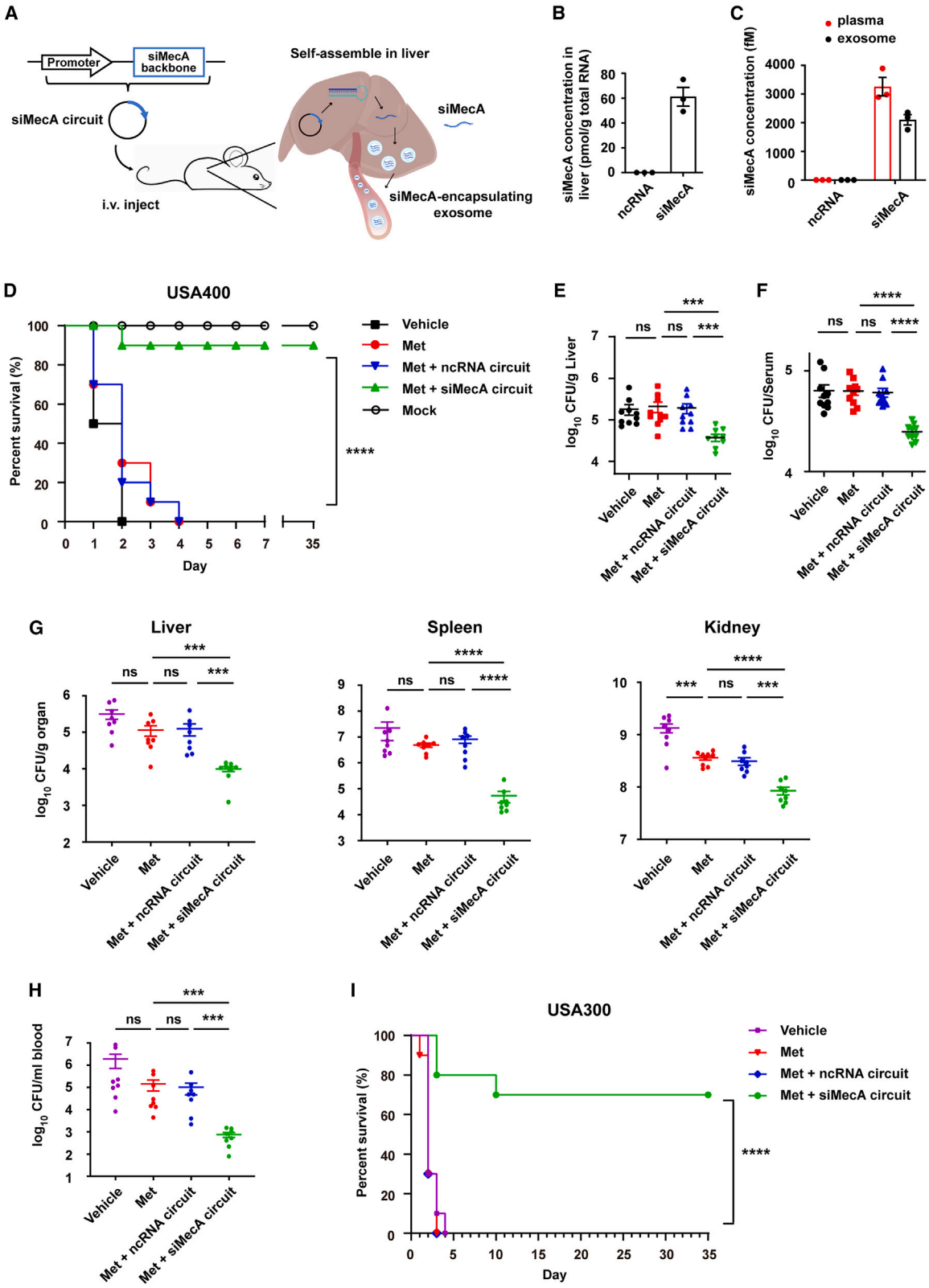

(legend on next page)

CellPress
OPEN ACCESS

DISCUSSION

Drug-resistant bacterial pathogens pose a major threat to public health, and the dense microbial population in the gut is connected to numerous processes related to human biology. Techniques to manipulate the behavior of interacting bacteria are urgently needed to facilitate the development of therapeutics for diseases related to microbiome dysfunction. Here, our study reveals that mammalian cell-derived exosomes are effective mediators of sRNA trafficking to bacteria *in vivo*, which subsequently induces bacterial gene silencing.

The RNAi pathway in mammalian cells requires RISC, especially the key protein AGO.[10] Although prokaryotic homologs of AGO proteins have been identified, they usually play roles in host defense by mediating the cleavage of exogenous DNA but not bacterial gene regulation.[34] Our study suggests that exosome-mediated bacterial gene silencing is mainly induced by the exosomal AGO2 protein as an exogenous gene regulatory protein. Interestingly, although the siRNAs used in this study are perfectly base paired with target bacterial genes, bacterial gene silencing appears to be a result of translational repression rather than endonucleolytic cleavage of mRNA, which is in striking contrast to what occurs in eukaryotic cells (Figure S14).[35] This raises two questions: first, why did AGO2 not cleave the target bacterial mRNA in the circumstance of perfect base-paring? Second, what is the mechanism of translational repression? Firstly, there must be unknown mechanisms that suppress the cleavage reaction: perhaps the cleavage activity of AGO2 is inhibited by bacterial proteins or steric hindrance, or mammalian AGO2 just cannot cleave bacterial mRNA. Secondly, translational repression without mRNA degradation is also observed in plants, although miRNAs perfectly match the target mRNAs. For example, plant miRNA can repress translation initiation and elongation of target RNAs without promoting deadenylation or mRNA decay[36]; plant 22-nt siRNAs, which are induced by environmental stress, repress the translation of target mRNAs[37]; a recent report has provided one explanation that in *Arabidopsis*, 22-nt small RNAs loaded into AGO1 recruit the plant-specific dsRNA-binding protein SGS3 and result in ribosome stalling on the target mRNAs.[38] Here, we hypothesize that the AGO2-siRNA complex may interact with other accessory proteins and block the occupancy of ribosomes or cause ribosome stalling, resulting in translation repression in bacteria. We have found that GW182 is necessary for siMecA-mediated gene silencing, but how it works may differ from that in mammals, which occurred in the initial step of translation and was related to deadenylation.[27] Our data did not exclude the possibility that unidentified bacterial proteins might function together with the AGO2 protein during bacterial gene silencing. As the pull-down assay showed, several staphylococcal proteins were likely to interact with siMecA and may participate in siMecA-mediated gene silencing. The altered regulatory behavior of AGO2 with perfectly matched sRNA in bacteria might be due to the participation of additional regulatory elements. It is likely that the siRNA-AGO2 complex that binds to the coding sequence of the target mRNA, possibly along with associated GW182 and specific bacterial proteins, imposes an extreme barrier for trailing ribosomes. This may partly explain why siRNAs can repress translation at the elongation step. Further investigation will be required to delineate the mechanisms. Overall, mammalian cell-derived exosomes not only transport sRNAs but also deliver RISC-related proteins as foreign regulatory machinery that controls intracellular processes into bacterial cells.

The transportation of regulatory biomolecules from pathogenic bacteria to eukaryotic cells is well characterized. *C. elegans* interprets bacterial non-coding RNAs to learn pathogenic avoidance.[39] A secreted bacterial RNA-binding protein, Zea, modulates the host retinoic acid-inducible gene I signaling.[40] However, the regulation of bacterial cells by biomolecules secreted by eukaryotic cells has been rarely reported. Our study shows that exosomes deliver both siRNAs and miRNAs

Figure 5. Intravenous injection of the siMecA circuit enhances the effect of methicillin treatment to protect mice from lethal MRSA infection

(A) Schematic description of *in vivo* self-assembled siMecA-Exos$_{mice}$. The siMecA circuit contains a promoter part and an siMecA-expressing part. When the siMecA circuit is taken up and processed by the liver after intravenous injection, the promoter drives the transcription of siMecA, which leads to the loading of saturated siMecA into exosomes as cargo. Subsequently, siMecA-encapsulating exosomes (siMecA-Exos$_{mice}$) facilitate the systematic distribution of siMecA to multiple organs.

(B) The expression level of siMecA in the mouse liver following tail vein injection of 5 mg/kg siMecA circuit (n = 3), as determined by qRT-PCR.

(C) The expression levels of siMecA in the mouse plasma and plasma exosomes following tail vein injection of the 5 mg/kg siMecA circuit (n = 3) were determined by qRT-PCR.

(D) Effects of methicillin and the siMecA circuit in protecting mice (n = 10) from lethal infection with 5 × 10^7 CFU of MRSA USA400 (MW2). Infected mice received 3 mg/kg methicillin by intraperitoneal (i.p.) injection and 5 mg/kg siMecA circuit by tail vein injection (i.v.) every day for 7 days. The asterisk indicates a significant difference between ncRNA circuit and siMecA circuit.

(E and F) Effect of methicillin and the siMecA circuit on *S. aureus* survival in the livers (E) and sera (F) (n = 10) of mice challenged with USA400 MW2 bacteria 24 h post infection. Each symbol represents the level in 1 g liver or 5 μL serum sample from an individual mouse. The horizontal bars indicate the mean values. The error bars indicate the SEM of total values.

(G and H) Effect of methicillin and the siMecA circuit on *S. aureus* survival in the organs (G, liver, spleen, and kidney) and blood (H) (n = 8) of mice challenged with 7.5 × 10^7 CFU of USA300. Infected mice received 6 mg/kg methicillin (i.p.) and 5 mg/kg siMecA circuit (i.v.) daily for 3 days, and then were killed the next day. Each symbol represents the level in 1 g tissue, or 1 mL blood sample from an individual mouse. The horizontal bars indicate the mean values. The error bars indicate the SEM of total values.

(I) Effects of methicillin and the siMecA circuit in protecting mice (n = 10) from lethal infection with 1 × 10^8 CFU of USA300. Infected mice received 6 mg/kg methicillin (i.p.) and 5 mg/kg siMecA circuit (i.v.) daily for 7 days. The asterisk indicates a significant difference between ncRNA circuit and siMecA circuit.

All data are means ± SEM. n = number of biological replicates. Statistical significance was determined using log rank test (D and I) and one-way ANOVA with Tukey's post hoc test (E–H). ***p < 0.001, ****p < 0.0001. ns, not significant. See also Figures S11–S13.

into bacteria (Table S3), and exosome-mediated RNAi may function with imperfectly matched sequences (Figures 2G and 2H; Figures 3J and 3K). We found that siMecA with 3-nt mismatches was still functional, a little weaker than the perfect match, and siMecA mutated at the 3′ end was more effective than that mutated at the 5′ end or in the middle. When the mismatch increased to 4-nt, only siAda mutated at the 3′ end was functional, and if the mismatch in siAda increased to 5-nt, the mutant can no longer downregulate the target gene, suggesting that the limit of mismatch may be 4-nt, and the base-paring between the 5′ end as well as the middle part of the siRNA and the target mRNA may be more critical. Based on the aforementioned findings, we speculate that exosomal miRNAs, which have multiple bacterial targets with imperfect base-paring, may regulate bacterial genes in the same way as exosomal siRNAs. Our study implies that exosome-mediated AGO2-sRNA transport and bacterial gene silencing is a potential pathway by which eukaryotic cells regulate interacting pathogenic bacteria *in vivo*, as demonstrated in the treatment of MRSA infection by mouse liver-produced siMecA-Exos$_{mice}$. It is intriguing to consider the possibility that mammalian hosts employ exosomes to transport molecules with biological functions to the mammalian microbiome for interspecies communication and regulation under physiological conditions.

Our study demonstrates the potential of this strategy in fighting pathogenic bacteria, such as MRSA, utilizing synthetic sRNAs that specifically target virulence and drug resistance genes. Such a strategy might offer an important advantage over traditional antibiotics, which require extensive chemical remodeling once mutations of the target bacterial proteins lead to drug resistance. By simply matching the sequences of synthetic sRNAs to target bacterial genes, exosome-mediated RNAi could overcome the resistance mutations of virulence and drug resistance genes in pathogenic bacteria. Combined with a synthetic biology technique that utilizes the host liver to produce circulating exosomes containing specific siRNA sequences, exosome-mediated bacterial gene regulation is a promising therapeutic strategy for treating diseases related to pathogenic infections. The genetic circuits are biocompatible, non-toxic, and non-immunogenic.[29] We have calculated the dose-effect relationship in the mouse model: 20 μg genetic circuits ≈ 100 μg exosome ≈ 25 siRNAs per bacterial cell, which helps to guide the dose for humans in the future.

Limitations of the study

The mechanism of the siRNA-AGO2 complex inhibiting bacterial protein translation needs further investigation. The electroporation of the siRNA-AGO2 complex into bacteria to confirm the mechanism is currently limited by existing techniques. Additionally, in the exosome purification method, treating the isolated exosomes with RNase and DNase to remove non-specifically bound nucleic acids would enhance the specificity of the results. Furthermore, it will be important to generalize our findings using a broader range of clinical strains and models. Since methicillin is rarely used in clinical settings at present, future studies will focus on utilizing clinically available antibiotics to ensure the practical relevance of our research.

RESOURCE AVAILABILITY

Lead contact

Further information and requests for resources and reagents should be directed to the lead contact, Huan Wang (wanghuan@nju.edu.cn).

Materials availability

This study did not generate any new unique reagents.

Data and code availability

- The sequencing dataset has been deposited in the GEO database (GEO: GSE122212).
- This paper does not report any original code.
- Any additional information required to reanalyze the data reported in this work paper is available from the lead contact upon request.

ACKNOWLEDGMENTS

We thank Dr. Yin Ding (State Key Laboratory of Analytical Chemistry for Life Science, Nanjing University) for technical help with imaging and Dr. Hao Zhang (EVLiXiR, Nanjing) for the help with exosome preparation and mass spectrometry. We thank Dr. Qipeng Zhang (School of Life Sciences, Nanjing University) for his help in statistical analysis. This work was supported by grants from the National Key R&D Program of China (2018YFA0507100) to K.Z., the National Natural Science Foundation of China (31601057 to C.W., 82473974 to H.B., and 22325702 to H.W.), Natural Science Foundation of Jiangsu Province (BK20232020) to H.W., the Fundamental Research Funds for the Central Universities (14380045 to C.W. and 14380138 and 14380131 to H.W.), and Senior Talent Foundation of Jiangsu University (5501290013 to C.W.).

AUTHOR CONTRIBUTIONS

C.-Y.Z., H.W., H.B., and C.W. designed and supervised this study. C.W., W.S., Y. Zhou, X.H., J.Z., Y.G., X.M., Y.B., W.L., Y. Zhang, L.Z., and J.Y. performed the experiments. C.W., H.W., C.-Y.Z., H.B., and H.L. analyzed the data. H.B., H.L., Y.X., T.X., and K.Z. contributed to the materials. Z.Z., X.L., and H.S. performed bioinformatics analysis. C.W., H.W., and C.-Y.Z. wrote the manuscript.

DECLARATION OF INTERESTS

C.-Y.Z., C.W., and H.W. are co-inventors on a patent application (PCT/CN2020/133392) related to this work.

STAR★METHODS

Detailed methods are provided in the online version of this paper and include the following:

- KEY RESOURCES TABLE
- EXPERIMENTAL MODEL AND STUDY PARTICIPANT DETAILS
  - Cell lines and microbe strains
  - Mice
- METHOD DETAILS
  - Transfection
  - Exosome purification
  - Nanoparticle tracking analysis (NTA)
  - Uptake of exosomes by bacteria by co-incubation
  - Quantitative reverse-transcription (RT) polymerase chain reaction (PCR)
  - Electroporation
  - Illumine HiSeq data analysis of exosomal miRNA
  - Confocal microscopy analysis
  - Immuno-TEM analysis
  - Western blot analysis
  - Immunoprecipitation assay
  - RNA pull-down assay
  - Northern blot analysis

- Minimum inhibitory concentration (MIC) assay
- Time-killing assays
- Mouse infection model
- Isolation of MRSA bacteria from serum/plasma of infected mice
- Construction and characterization of the siMecA circuit
- Calculation of sRNA content in bacteria and medium

- QUANTIFICATION AND STATISTICAL ANALYSIS

SUPPLEMENTAL INFORMATION

Supplemental information can be found online at https://doi.org/10.1016/j.xcrm.2025.101997.

Received: May 5, 2023
Revised: October 15, 2024
Accepted: February 11, 2025
Published: March 6, 2025

REFERENCES

1. Bush, K., Courvalin, P., Dantas, G., Davies, J., Eisenstein, B., Huovinen, P., Jacoby, G.A., Kishony, R., Kreiswirth, B.N., Kutter, E., et al. (2011). Tackling antibiotic resistance. Nat. Rev. Microbiol. *9*, 894–896. https://doi.org/10.1038/nrmicro2693.
2. Payne, D.J., Gwynn, M.N., Holmes, D.J., and Pompliano, D.L. (2007). Drugs for bad bugs: confronting the challenges of antibacterial discovery. Nat. Rev. Drug Discov. *6*, 29–40. https://doi.org/10.1038/nrd2201.
3. Hatfull, G.F., Dedrick, R.M., and Schooley, R.T. (2022). Phage Therapy for Antibiotic-Resistant Bacterial Infections. Annu. Rev. Med. *73*, 197–211. https://doi.org/10.1146/annurev-med-080219-122208.
4. Yan, Q., and Fong, S.S. (2017). Challenges and Advances for Genetic Engineering of Non-model Bacteria and Uses in Consolidated Bioprocessing. Front. Microbiol. *8*, 2060. https://doi.org/10.3389/fmicb.2017.02060.
5. Monk, I.R., Shah, I.M., Xu, M., Tan, M.W., and Foster, T.J. (2012). Transforming the untransformable: application of direct transformation to manipulate genetically *Staphylococcus aureus* and *Staphylococcus epidermidis*. mBio *3*, e00277. https://doi.org/10.1128/mBio.00277-11.
6. Ghildiyal, M., and Zamore, P.D. (2009). Small silencing RNAs: an expanding universe. Nat. Rev. Genet. *10*, 94–108. https://doi.org/10.1038/nrg2504.
7. Ipsaro, J.J., and Joshua-Tor, L. (2015). From guide to target: molecular insights into eukaryotic RNA-interference machinery. Nat. Struct. Mol. Biol. *22*, 20–28. https://doi.org/10.1038/nsmb.2931.
8. Kuhn, C.-D., and Joshua-Tor, L. (2013). Eukaryotic Argonautes come into focus. Trends Biochem. Sci. *38*, 263–271. https://doi.org/10.1016/j.tibs.2013.02.008.
9. Setten, R.L., Rossi, J.J., and Han, S.-p. (2019). The current state and future directions of RNAi-based therapeutics. Nat. Rev. Drug Discov. *18*, 421–446. https://doi.org/10.1038/s41573-019-0017-4.
10. Shabalina, S.A., and Koonin, E.V. (2008). Origins and evolution of eukaryotic RNA interference. Trends Ecol. Evol. *23*, 578–587. https://doi.org/10.1016/j.tree.2008.06.005.
11. van Niel, G., D'Angelo, G., and Raposo, G. (2018). Shedding light on the cell biology of extracellular vesicles. Nat. Rev. Mol. Cell Biol. *19*, 213–228. https://doi.org/10.1038/nrm.2017.125.
12. Zhou, G., and Chen, X. (2019). Emerging role of extracellular microRNAs and lncRNAs. ExRNA *1*, 10. https://doi.org/10.1186/s41544-019-0012-2.
13. Schwechheimer, C., and Kuehn, M.J. (2015). Outer-membrane vesicles from Gram-negative bacteria: biogenesis and functions. Nat. Rev. Microbiol. *13*, 605–619. https://doi.org/10.1038/nrmicro3525.
14. Chen, X., Ba, Y., Ma, L., Cai, X., Yin, Y., Wang, K., Guo, J., Zhang, Y., Chen, J., Guo, X., et al. (2008). Characterization of microRNAs in serum: a novel class of biomarkers for diagnosis of cancer and other diseases. Cell Res. *18*, 997–1006. https://doi.org/10.1038/cr.2008.282.
15. Zhang, Y., Liu, D., Chen, X., Li, J., Li, L., Bian, Z., Sun, F., Lu, J., Yin, Y., Cai, X., et al. (2010). Secreted Monocytic miR-150 Enhances Targeted Endothelial Cell Migration. Mol. Cell *39*, 133–144. https://doi.org/10.1016/j.molcel.2010.06.010.
16. Lv, Z., Wei, Y., Wang, D., Zhang, C.-Y., Zen, K., and Li, L. (2014). Argonaute 2 in Cell-Secreted Microvesicles Guides the Function of Secreted miRNAs in Recipient Cells. PLoS One *9*, e103599. https://doi.org/10.1371/journal.pone.0103599.
17. McKenzie, A.J., Hoshino, D., Hong, N.H., Cha, D.J., Franklin, J.L., Coffey, R.J., Patton, J.G., and Weaver, A.M. (2016). KRAS-MEK Signaling Controls Ago2 Sorting into Exosomes. Cell Rep. *15*, 978–987. https://doi.org/10.1016/j.celrep.2016.03.085.
18. Mielecki, D., Wrzesiński, M., and Grzesiuk, E. (2015). Inducible repair of alkylated DNA in microorganisms. Mutat. Res. Rev. Mutat. Res. *763*, 294–305. https://doi.org/10.1016/j.mrrev.2014.12.001.
19. Li, J., Chen, X., Yi, J., Liu, Y., Li, D., Wang, J., Hou, D., Jiang, X., Zhang, J., Wang, J., et al. (2016). Identification and Characterization of 293T Cell-Derived Exosomes by Profiling the Protein, mRNA and MicroRNA Components. PLoS One *11*, e0163043. https://doi.org/10.1371/journal.pone.0163043.
20. Kadurugamuwa, J.L., and Beveridge, T.J. (1996). Bacteriolytic effect of membrane vesicles from *Pseudomonas aeruginosa* on other bacteria including pathogens: conceptually new antibiotics. J. Bacteriol. *178*, 2767–2774. https://doi.org/10.1128/jb.178.10.2767-2774.1996.
21. Morita, T., Mochizuki, Y., and Aiba, H. (2006). Translational repression is sufficient for gene silencing by bacterial small noncoding RNAs in the absence of mRNA destruction. Proc. Natl. Acad. Sci. USA *103*, 4858–4863. https://doi.org/10.1073/pnas.0509638103.
22. De Lay, N., Schu, D.J., and Gottesman, S. (2013). Bacterial Small RNA-based Negative Regulation: Hfq and Its Accomplices. J. Biol. Chem. *288*, 7996–8003. https://doi.org/10.1074/jbc.R112.441386.
23. Rivas, F.V., Tolia, N.H., Song, J.-J., Aragon, J.P., Liu, J., Hannon, G.J., and Joshua-Tor, L. (2005). Purified Argonaute2 and an siRNA form recombinant human RISC. Nat. Struct. Mol. Biol. *12*, 340–349. https://doi.org/10.1038/nsmb918.
24. Meister, G., Landthaler, M., Patkaniowska, A., Dorsett, Y., Teng, G., and Tuschl, T. (2004). Human Argonaute2 Mediates RNA Cleavage Targeted by miRNAs and siRNAs. Mol. Cell *15*, 185–197. https://doi.org/10.1016/j.molcel.2004.07.007.
25. DeLeo, F.R., and Chambers, H.F. (2009). Reemergence of antibiotic-resistant *Staphylococcus aureus* in the genomics era. J. Clin. Investig. *119*, 2464–2474. https://doi.org/10.1172/JCI38226.
26. Pantosti, A., Sanchini, A., and Monaco, M. (2007). Mechanisms of antibiotic resistance in *Staphylococcus aureus*. Future Microbiol. *2*, 323–334. https://doi.org/10.2217/17460913.2.3.323.
27. Iwakawa, H.-o., and Tomari, Y. (2015). The Functions of MicroRNAs: mRNA Decay and Translational Repression. Trends Cell Biol. *25*, 651–665. https://doi.org/10.1016/j.tcb.2015.07.011.
28. György, B., Hung, M.E., Breakefield, X.O., and Leonard, J.N. (2015). Therapeutic Applications of Extracellular Vesicles: Clinical Promise and Open Questions. Annu. Rev. Pharmacol. Toxicol. *55*, 439–464. https://doi.org/10.1146/annurev-pharmtox-010814-124630.
29. Fu, Z., Zhang, X., Zhou, X., Ur-Rehman, U., Yu, M., Liang, H., Guo, H., Guo, X., Kong, Y., Su, Y., et al. (2021). *In vivo* self-assembled small RNAs as a new generation of RNAi therapeutics. Cell Res. *31*, 631–648. https://doi.org/10.1038/s41422-021-00491-z.
30. Liu, F., Song, Y., and Liu, D. (1999). Hydrodynamics-based transfection in animals by systemic administration of plasmid DNA. Gene Ther. *6*, 1258–1266. https://doi.org/10.1038/sj.gt.3300947.
31. Zhang, G., Budker, V., and Wolff, J.A. (1999). High levels of foreign gene expression in hepatocytes after tail vein injections of naked

plasmid DNA. Hum. Gene Ther. *10*, 1735–1737. https://doi.org/10.1089/10430349950017734.

32. Li, J., Zhang, Y., Liu, Y., Dai, X., Li, W., Cai, X., Yin, Y., Wang, Q., Xue, Y., Wang, C., et al. (2013). Microvesicle-mediated Transfer of MicroRNA-150 from Monocytes to Endothelial Cells Promotes Angiogenesis. J. Biol. Chem. *288*, 23586–23596. https://doi.org/10.1074/jbc.M113.489302.
33. Fong, M.Y., Zhou, W., Liu, L., Alontaga, A.Y., Chandra, M., Ashby, J., Chow, A., O'Connor, S.T.F., Li, S., Chin, A.R., et al. (2015). Breast-cancer-secreted miR-122 reprograms glucose metabolism in premetastatic niche to promote metastasis. Nat. Cell Biol. *17*, 183–194. https://doi.org/10.1038/ncb3094.
34. Olovnikov, I., Chan, K., Sachidanandam, R., Newman, D.K., and Aravin, A.A. (2013). Bacterial Argonaute Samples the Transcriptome to Identify Foreign DNA. Mol. Cell *51*, 594–605. https://doi.org/10.1016/j.molcel.2013.08.014.
35. El Andaloussi, S., Lakhal, S., Mäger, I., and Wood, M.J.A. (2013). Exosomes for targeted siRNA delivery across biological barriers. Adv. Drug Deliv. Rev. *65*, 391–397. https://doi.org/10.1016/j.addr.2012.08.008.
36. Iwakawa, H.O., and Tomari, Y. (2013). Molecular insights into microRNA-mediated translational repression in plants. Mol. Cell *52*, 591–601. https://doi.org/10.1016/j.molcel.2013.10.033.
37. Wu, H., Li, B., Iwakawa, H.O., Pan, Y., Tang, X., Ling-Hu, Q., Liu, Y., Sheng, S., Feng, L., Zhang, H., et al. (2020). Plant 22-nt siRNAs mediate translational repression and stress adaptation. Nature *581*, 89–93. https://doi.org/10.1038/s41586-020-2231-y.
38. Iwakawa, H.O., Lam, A.Y.W., Mine, A., Fujita, T., Kiyokawa, K., Yoshikawa, M., Takeda, A., Iwasaki, S., and Tomari, Y. (2021). Ribosome stalling caused by the Argonaute-microRNA-SGS3 complex regulates the production of secondary siRNAs in plants. Cell Rep. *35*, 109300. https://doi.org/10.1016/j.celrep.2021.109300.
39. Kaletsky, R., Moore, R.S., Vrla, G.D., Parsons, L.R., Gitai, Z., and Murphy, C.T. (2020). *C. elegans* interprets bacterial non-coding RNAs to learn pathogenic avoidance. Nature *586*, 445–451. https://doi.org/10.1038/s41586-020-2699-5.
40. Pagliuso, A., Tham, T.N., Allemand, E., Robertin, S., Dupuy, B., Bertrand, Q., Bécavin, C., Koutero, M., Najburg, V., Nahori, M.A., et al. (2019). An RNA-Binding Protein Secreted by a Bacterial Pathogen Modulates RIG-I Signaling. Cell Host Microbe *26*, 823–835. https://doi.org/10.1016/j.chom.2019.10.004.
41. Baba, T., Takeuchi, F., Kuroda, M., Yuzawa, H., Aoki, K.-i., Oguchi, A., Nagai, Y., Iwama, N., Asano, K., Naimi, T., et al. (2002). Genome and virulence determinants of high virulence community-acquired MRSA. Lancet *359*, 1819–1827. https://doi.org/10.1016/S0140-6736(02)08713-5.
42. Jia, J., Zheng, M., Zhang, C., Li, B., Lu, C., Bai, Y., Tong, Q., Hang, X., Ge, Y., Zeng, L., et al. (2023). Killing of *Staphylococcus aureus* persisters by a multitarget natural product chrysomycin A. Sci. Adv. *9*, eadg5995. https://doi.org/10.1126/sciadv.adg5995.
43. Langmead, B., Trapnell, C., Pop, M., and Salzberg, S.L. (2009). Ultrafast and memory-efficient alignment of short DNA sequences to the human genome. Genome Biol. *10*, R25. https://doi.org/10.1186/gb-2009-10-3-r25.
44. Rehmsmeier, M., Steffen, P., Höechsmann, M., and Giegerich, R. (2004). Fast and effective prediction of microRNA/target duplexes. RNA *10*, 1507–1517. https://doi.org/10.1261/rna.5248604.
45. Chen, F., Di, H., Wang, Y., Cao, Q., Xu, B., Zhang, X., Yang, N., Liu, G., Yang, C.-G., Xu, Y., et al. (2016). Small-molecule targeting of a diapophytoene desaturase inhibits *S. aureus* virulence. Nat. Chem. Biol. *12*, 174–179. https://doi.org/10.1038/nchembio.2003.

CellPress
OPEN ACCESS

STAR★METHODS

KEY RESOURCES TABLE

REAGENT or RESOURCE	SOURCE	IDENTIFIER
Antibodies		
Anti-AGO2	Abcam	Cat# ab57113; RRID: AB_2230916
Anti-AGO2	Abcam	Cat# ab32381; RRID: AB_867543
Anti-CD63	Abcam	Cat# ab134045; RRID: AB_2800495
Anti-Ada	Abcam	Cat# ab18104; RRID: AB_444248
Anti-DnaK	Abcam	Cat# ab69617; RRID: AB_1209209
Anti-PBP2a	BBI Solutions	Cat# BM306-F9D5
Anti-GW182	Bethyl	Cat# A302-329A; RRID: AB_1850240
Anti-β-actin	Santa Cruz	Cat# sc-47778; RRID: AB_626632
Anti-GAPDH	Invitrogen	Cat# MA5-15738, RRID: AB_10977387
Mouse normal IgG	BioVision	Cat# 1265
Rabbit normal IgG	Proteintech	Cat# B900610; RRID: AB_3674206
Bacterial and virus strains		
Escherichia coli BL21 (DE3)	Invitrogen	Cat# C600003
methicillin-resistant *Staphylococcus aureus* (MRSA) USA400 MW2	Hong Ling Lab[41]	N/A
MRSA USA300	Hongkai Bi Lab[42]	N/A
MRSA BHKS717	Hongkai Bi Lab[42]	N/A
Chemicals, peptides, and recombinant proteins		
Methicillin Sodium	USP	Cat# 1410002
Lysozyme	BBI	Cat# A610308
Lysostaphin	BBI	Cat# A619001
Protein A/G-Agarose	Santa Cruz	Cat# sc-2003
10nm Protein-A/Gold particle	AURION	Cat# 25285
Protease Inhibitor Cocktail	Thermo Scientific	Cat# 88669
RNase Inhibitor	Takara	Cat# 2313A
TSB broth	Difco	Cat# 286220
Lipofectamine 2000	Invitrogen	Cat# 11668019
TRIzol Reagent	Invitrogen	Cat# 15596018
2×RNA loading buffer	Takara	Cat# 9168
PKH67	Sigma	Cat# PKH67GL
FM4-64	Invitrogen	Cat# T13320
DAPI	Beyotime	Cat# C1002
Coomassie blue	Beyotime	Cat# ST031
Critical commercial assays		
exosome isolation kit	Invitrogen	Cat# 4478359
Mouse TNF-α ELISA KIT	4A Biotech	Cat# CME0004
Mouse IL-6 ELISA KIT	4A Biotech	Cat# CME0006
TaqMan probes	Applied Biosystems	Cat# 4440887
miRCURY LNA custom detection probe	Qiagen	Cat# 339115
miRNeasy Mini Kit	Qiagen	Cat# 217004
DIG Easy Hyb solution	Roche	Cat# 11796895001
DIG Luminescent Detection Kit	Roche	Cat# 1363514
Deposited data		
Illumine HiSeq data	This paper	GEO: GSE122212

(*Continued on next page*)

Continued

REAGENT or RESOURCE	SOURCE	IDENTIFIER
Experimental models: Cell lines		
Human: HEK293T	Stem Cell Bank, Chinese Academy of Sciences	SCSP-502
Human: A549	Stem Cell Bank, Chinese Academy of Sciences	SCSP-503
Human: SW480	Stem Cell Bank, Chinese Academy of Sciences	SCSP-5033
Human: TE-10	Stem Cell Bank, Chinese Academy of Sciences	TCHu 90
Human: Caco-2	Stem Cell Bank, Chinese Academy of Sciences	SCSP-5027
Human: SGC-7901	Stem Cell Bank, Chinese Academy of Sciences	TCHu 46
Experimental models: Organisms/strains		
Mouse: BALB/c	Animal Core Facility of Nanjing Medical University	N/A
Oligonucleotides		
See Table S1 for siRNAs	RiboBio	N/A
See Table S1 for qRT-PCR primers	Genscript	N/A
Recombinant DNA		
ada-pET-28a	This paper	N/A
mecA-pcDNA3.1	This paper	N/A
ncRNA circuit	GenePharma	C02007
siMecA circuit	This paper	N/A
Software and algorithms		
bowtie	Langmead et al.[43]	http://bowtie-bio.sourceforge.net/index.shtml
RNAhybrid	Rehmsmeier et al.[44]	https://bibiserv.cebitec.uni-bielefeld.de/rnahybrid/
GraphPad Prism v9.0	GraphPad software	https://www.graphpad.com
ImageJ	NIH	https://imagej.net/ij/

EXPERIMENTAL MODEL AND STUDY PARTICIPANT DETAILS

Cell lines and microbe strains

Human HEK293T, A549, SW480, TE-10, Caco-2 and SGC-7901 cells were purchased from the China Cell Culture Center (Shanghai, China), and cultured according to the instruction. All cell lines were characterized by short tandem repeat analysis and Mycoplasma testing. The *E. coli* BL21 (DE3) strain was purchased from Invitrogen (Carlsbad, CA, USA). The community-associated methicillin-resistant *Staphylococcus aureus* (CA-MRSA) USA400 (MW2) was a standard strain whose genome has been sequenced,[41] and was obtained from Harbin Medical University as a kind gift. USA300 (a standard MRSA strain) and BHKS717 (a clinical isolate MRSA strain)[42] were provided by Dr. Hongkai Bi (Nanjing Medical University). MRSA strain was grown in tryptic soy broth (TSB) or on tryptic soy agar (TSA) plates. *E. coli* BL21 (DE3) was grown in Luria Bertani (LB) broth or on LB agar plates.

Mice

6-8-week-old female BALB/c mice were obtained from Nanjing Medical University (NJMU, Nanjing, China) and housed under specified pathogen-free conditions. The animals received humane care according to the guidelines approved by Animal Ethical and Welfare Committee of NJMU.

METHOD DETAILS

Transfection

HEK-293T cells were seeded on a 225-cm^2 flask. When cells reached approximately 80% confluence next day, they were transfected with synthetic double-stranded siRNAs using Lipofectamine 2000 (Invitrogen). Briefly, 5 mL of siRNA-lipofectamine (lipo) mixture was

produced by incubating 112.5 μL lipo with 2.25 nmol of siRNA, at room temperature (r.t.) for 15 min. Before transfection, cell culture medium was exchanged to Opti-MEM medium (Gibco, 31985). The cells were incubated with the transfection mixture for 6 h at 37°C and 5% CO_2. Subsequently, the medium was discarded, followed by two washes with PBS to remove excess transfection mixture, and exchanged for fresh DMEM medium containing 2% exosome-depleted fetal bovine serum (FBS), which was centrifuged at 100,000 g overnight to wipe out the existing exosomes, or purchased from VivaCell (Cat# C38010050). The culture was further incubated for 24 h allowing for the production of engineered exosomes, and then the supernatant was collected to harvest exosomes.

Exosome purification

Exosomes were purified by ultracentrifugation, or using a Total Exosome Isolation Reagent (from cell culture media) from Invitrogen (Cat #4478359) according to the manufacturer's instructions. Briefly, the cell culture medium was sequentially centrifuged at 300×g for 5 min and 3,000×g for 25 min to remove cells and cell debris, followed by centrifugation at 10,000×g for 60 min to get rid of large-size vesicles such as apoptotic bodies. The resulting supernatant was either subjected to ultracentrifugation, or added with 0.5 volumes of the isolation reagent, mixed, and incubated at 4°C overnight. The reagent is a proprietary polymer that gently precipitates exosomes, by tying up water molecules, it forces less-soluble components such as vesicles out of solution, allowing them to be collected by a short, low-speed centrifugation. The sample was then centrifuged at 10,000 × g for 1 h at 4°C, with exosomes contained in the pellet. Then, exosomes were washed with PBS and recovered by centrifugation at 100,000 g for 1 h. Finally, exosomes were resuspended in PBS and filtered through a syringe filter (0.2 μm) to prevent aggregation of exosomes and to remove excess polymers. The purified exosomes were characterized by NTA, EM and western blot analysis of marker proteins to ensure that the quality of exosomes from each batch is consistent.

Nanoparticle tracking analysis (NTA)

Typically, exosomes were resuspended in phosphate buffer saline (PBS) to a concentration of 5 μg of protein/ml, diluted by 100- to 500-fold, passed through a 0.2 μm filter, and analyzed by the Nanosight NS 300 system (NanoSight).

Uptake of exosomes by bacteria by co-incubation

Typically, overnight cultures of bacteria were diluted in fresh culture medium, with the initial number to be approximately 2×10^7. Exosomes were then added to the bacterial culture at concentrations of 50, 100, 200 μg/mL total protein, as quantified by BCA protein assay (exact siRNA concentration was also indicated in the figure legend), and incubated for indicated time in a shaking incubator at 37°C. After exosome incubation, the pellet of bacterial cells was washed with PBS containing 0.1% Triton X-100 to remove excess exosomes.

Quantitative reverse-transcription (RT) polymerase chain reaction (PCR)

Total RNA extracted from cells, tissues or bacteria was typically isolated using TRIzol Reagent. Total RNA from serum, exosomes or IP products was extracted using the miRNeasy Mini Kit. qRT-PCR was performed on an ABI7500 (Applied Biosystems). TaqMan probes for siRNAs and miRNAs were purchased from Applied Biosystems (Foster City, CA, USA).

To calculate the absolute amount of sRNAs in exosomes and bacteria, a series of synthetic small RNAs of known concentrations were also subject to qRT-PCR, by which a standard curve was generated. The quantification of small RNAs was then calculated in reference to the standard curve. The sRNA content in the cells and tissues was normalized to U6 snRNA. Expression levels of *ada* and *mecA* mRNAs in bacteria were normalized to 16S rRNA levels using the $2^{-\Delta\Delta Ct}$ method. The experiments were performed in triplicate.

Electroporation

5 pmol of siAda antisense was mixed with 50 μL of electro-competent *E. coli* bacteria (8×10^8 CFU). Electroporation was carried out using 1 mm electroporation cuvette (Bio-Rad) in a MicroPulsor (Bio-Rad) at 2.5kV, 200Ω, 25μF, 5ms. Subsequently, samples were diluted to 2×10^7/mL *E. coli* in LB medium and cultured for 6 h.

Illumine HiSeq data analysis of exosomal miRNA

The sRNA libraries were made using Illumina TruSeq Small RNA Sample Prep Kits and sequenced on an Illumina HiSeq system by BGI (Shenzhen, China). After preprocessed with the procedure of quality control and adapter trimming, the clean reads were compared to known miRNA precursors from the miRBase database v21.0 to identify human miRNAs using bowtie.[43] Candidate reads with no more than 1 mismatch and 2nt shift in mature miRNA position were identified as mature miRNAs. The read numbers of miRNA in each library were normalized by the total number of miRNA reads, resulting in reads per million (RPM) normalized measurements. Top 100 abundant miRNAs in exosomes library were listed in Table S2. For *E. coli* library, the list of miRNAs was shown in Table S3, using 30 normalized RPM miRNA reads as a cutoff. In bacteria libraries, the normalized reads number of selected miRNAs must be 10 times higher than that in the control libraries. All data have been uploaded to the GEO database (GEO accession number: GSE122212).

The bacterial target gene prediction for human miRNAs was performed using RNAhybrid.[44]

Confocal microscopy analysis

293T cells were labeled with PKH67 for 5 min and then washed for three times with HBSS. The cells were cultured overnight in DMEM medium. The supernatants were then collected and centrifuged to harvest labeled exosomes.

E. coli was aerobically cultured at 37°C with 220 rpm shaking for 4 h in the presence of 200 μg/mL of Cy3-conjugated siAda-containing exosomes, or PKH67-labeled exosomes. After culturing, bacterial cells were washed with ice-cold PBS and fixed with ice-cold 2% paraformaldehyde (PFA). The bacterial cells were then stained with DAPI and subjected to confocal microscopy analysis with a 100× objective.

Immuno-TEM analysis

E. coli cells were fixed in a mixture of 4% PFA and 0.5% glutaraldehyde for 30 min at r.t. and 1 h on ice. After three washes in 0.1 M sodium cacodylate buffer, *E. coli* cells were dehydrated in ethanol, infiltrated with HM20 epoxy resin mixed with ethanol. *E. coli* cells were then embedded in pure, fresh HM20 epoxy resin and polymerized. Ultrathin sections (70 nm) were cut using a Leica ultra-microtome and placed onto a 300-mesh carbon/formvar coated grids. For immunogold staining, the grids were placed into a blocking buffer for a block/permeabilization step for 1 h and immediately incubated with the primary antibody (AGO2, ab57113, Abcam; CD63, ab134045, Abcam) at appropriate concentrations overnight at 4°C. Subsequently, grids were rinsed with PBS/0.1% Tween, floated on drops of 10 nm Protein-A/Gold particles (AURION, Hatfield, PA, USA) for 1 h at r.t. The grids were rinsed again with PBS/0.1% Tween and placed in 2.5% Glutaraldehyde in PBS for 5 min. After rinsed by distilled water, the grids were stained for contrast using uranyl acetate, dried, and analyzed with a Tecnai Spirit transmission electron microscope (FEI, Hillsboro, OR).

Western blot analysis

Protein samples were loaded onto polyacrylamide gels and transferred onto PVDF membranes (Millipore) by wet electrophoretic transfer. Blots were blocked for 1 h at r.t. with 5% non-fat dry milk in Tris-buffered saline (TBS)/0.1% Tween, and incubated overnight at 4°C with the primary antibodies. Secondary antibodies were incubated for 1 h. Blots were developed with chemiluminescent reagents from Pierce. For *E. coli* samples, DnaK protein was used as a loading control. For MRSA samples, Coomassie protein stain was used for loading control. The quantification was achieved by ImageJ software.

Immunoprecipitation assay

Exosomes were lysed with lysis buffer (20 mM Tris-HCl, 150 mM NaCl, 1% NP-40, 1 mM EDTA, 0.5 mM DTT, 1 mM NaF, 1 mM $MgCl_2$, Protease Inhibitor Cocktail, and RNase Inhibitor, pH 7.5) for 30 min on ice. The resulting lysates were cleared by centrifugation at 16,000 ×g for 10 min at 4°C, and then immunoprecipitated with mouse anti-AGO2 antibody (ab57113, Abcam) or mouse normal IgG (Cat #1265, BioVision). Suspensions were gently rocked at 4°C overnight, followed by Protein A/G-Agarose beads (sc-2003, Santa Cruz Biotechnology) incubation for 4 h. After centrifugation, the supernatant was discarded, and the Agarose beads were washed for three times with ice-cold lysis buffer. After the elution from the beads, the RNA components were extracted using a miRNeasy Mini Kit and analyzed by qRT-PCR. Proteins were detected by western blot using a rabbit anti-AGO2 antibody (ab32381, Abcam).

For *E. coli* samples, cells were resuspended in lysis buffer A (10 mM Tris-HCl, 20% sucrose, 50 mM NaCl, Protease Inhibitor Cocktail, and RNase Inhibitor, pH 8.0) supplemented with lysozyme (BBI, A610308), and incubated at 37°C for 30 min. The resulting sample was further treated by triple volume of lysis buffer B (50 mM HEPES-KOH, 150 mM NaCl, 1% NP-40, 1 mM EDTA, 0.5 mM DTT, 1 mM NaF, 1 mM $MgCl_2$, Protease Inhibitor Cocktail, and RNase Inhibitor, pH 7.5) and incubated on ice for 30 min. The cell lysates were cleared by centrifugation at 21,000 ×g for 15 min at 4°C.

For MRSA, lysis buffer A was further supplemented with lysostaphin (BBI, A619001) based on the recipe of the *E. coli* lysis buffer.

RNA pull-down assay

293T cells were transfected with biotin-labeled siMecA and exosomes containing siMecA-biotin (siMecA-biotin Exos) were isolated from the cell culture medium. MRSA was incubated with siMecA-biotin Exos. The resulting bacterial cells were crosslinked with 1% formaldehyde. Then the bacteria were resuspended in lysis buffer A supplemented with Lysostaphin, incubated at 37°C for 15 min to break down the cell wall, followed by adding triple volume of lysis buffer B and ultrasonic lysis. The cell lysates were cleared by centrifugation at 12,000 ×g for 15 min at 4°C, and then incubated with streptavidin beads on a rotator at 4°C for 4 h. After incubation, RNA–protein complexes were retrieved by streptavidin beads, washed five times in buffer B, and eluted in EB solution (1% SDS, 0.1M $NaHCO_3$). The crosslinks were reversed by 5 M NaCl. siMecA was examined by qRT-PCR to confirm pull-down efficiency. The binding proteins were separated by SDS-PAGE and visualized by silver staining. Protein bands presented only in the siMecA-biotin Exos-treated sample but not in the control sample (NC) were excised and identified by mass spectrometry. Staphylococcal proteins identified by the pull-down assay were shown in Table S4.

Northern blot analysis

RNA samples were extracted from 50 μg of siAda-Exo, and 5×10^8 *E coli* incubated with or without siAda-Exo. Synthetic siAda (10^{-2}-10^{-6} pmol) was used as a control. All samples were dissolved in 2× RNA loading buffer, heated at 65°C for 10 min, fractionated by 15% denaturing TBE-urea polyacrylamide gel, and then transferred onto a nylon membrane (Hybond-N+, Amersham, GE, USA) by

blotting at 250 mA in 0.5× TBE buffer for 1 h. The membrane was cross-linked, dried, and pre-hybridized by incubation in 10 mL of DIG Easy Hyb solution at 37°C for 30 min. The DIG-labeled LNA probe designed for siAda (Qiagen, Germantown, MD, USA) was added to the DIG Easy Hyb solution, and the membrane was incubated overnight at 55°C with rotation in a hybridization oven. After hybridization, the membrane was washed in 2× SSC (0.5% SDS), and then 0.5× SSC (0.5% SDS) for three times. Probe detection was performed using the DIG Luminescent Detection Kit. Briefly, the blots were incubated in blocking solution for 30 min and then in anti-DIG-AP antibody solution for 1 h, followed by three washes. After equilibration, the blots were incubated with the chemiluminescent substrate CSPD and exposed to Kodak X-OMAT BT film.

Minimum inhibitory concentration (MIC) assay

The MIC was determined by a broth microdilution assay following the CLSI (Clinical and Laboratory Standards Institute) method (M07-A10). 2-fold serial dilutions of methicillin (Cat #1410002, USP) were prepared in a 96-well microtiter plate containing 100 μL of media. MRSA cultures were grown at 37°C in MH broth to midlogarithmic phase (OD_{600} = 0.4 to 0.6) and diluted to give a final concentration of approximately 1 × 10^5 CFU/mL. Exosomes were added into the broth to 100 μg/mL. After incubation at 37°C with shaking for 24 h, the dilution series were analyzed for microbial growth. The MIC was defined as the lowest concentrations of methicillin with no visible growth of bacteria. All MIC assays were repeated with three independent experiments.

Time-killing assays

An overnight culture of MRSA was diluted in LB broth and grown to midlogarithmic phase at 37°C. Cells were then diluted to 1 × 10^6 CFU/mL in LB broth containing 1×MIC of methicillin. Exosomes were added to a concentration of 250 μg/mL. Subsequently, cells were incubated at 37°C with shaking, and serial dilutions were plated on LB agar plates at indicated time points for the determination of viable cells (CFU/mL). Each assay was repeated with three independent experiments.

Mouse infection model

Overnight cultures of MRSA strain were washed and diluted 100-fold in fresh TSB medium. The liquid culture was grown to mid-exponential phase at 37°C for about 3 h with shaking ($OD_{600} \approx 0.4$), 250 rpm of aeration, and then the bacteria were harvested and washed twice with ice-cold PBS. Colony forming units (CFUs) per milliliter was determined before mice were inoculated.

To evaluate the efficacy of exosomes, female BALB/c mice were infected by retro-orbital injection with 5 × 10^7 CFU of MRSA USA400 MW2 bacteria (day 0) following published literature.[45] Infected mice immediately received a daily dose of 3 mg/kg methicillin dissolved in sterile PBS by intra-peritoneal injection and 5 mg/kg of exosomes by tail-vein injection for 7 consecutive days (day 0–6). In the case of *in vivo* self-assembled siMecA-Exo_{mice}, mice received first intravenous dose of 5 mg/kg siMecA circuit 9 h before infection, allowing time for siMecA-$Exos_{mice}$ production, and subsequent daily dosing of 3 mg/kg methicillin and 5 mg/kg siMecA circuit after infection for 7 consecutive days. Mice were monitored for 35 days to evaluate survival. The log rank test was used to analyze mortality data.

To examine bacteria survival in the serum and tissues of infected mice that received different treatments, animals were killed 24 h post-infection (day 1). Serum was extracted, and organs (liver, spleen and kidney) from each mouse were aseptically removed and homogenized in PBS to obtain single-cell suspensions. Serial dilutions of each sample were plated on TSA plates for the enumeration of CFUs (n = 10). Statistical significance was determined by One-way ANOVA with Tukey's multiple hoc test.

To evaluate the severity of infection, amounts of inflammation cytokines (TNF-α and IL-6) in the serum of infected mice that received different treatments, as well as healthy mice (mock) were examined by ELISA 24 h post-infection (n = 5), using ELISA Kits (4A Biotech, Beijing, China).

In addition, USA300 strain was used to infect mice to examine the therapeutic effect of *in vivo* self-assembled siMecA-Exo_{mice} initiated by siMecA circuit. There are some modifications as below:

For the lethal challenge experiments, mice were infected with 1 × 10^8 CFU of USA300. The daily dose of methicillin for USA300 was 6 mg/kg.

To evaluate the efficacy of siMecA-Exos combined with methicillin on reducing the bacterial loads in blood and organs, mice were challenged with 7.5 × 10^7 CFU. Animals were killed after three consecutive days of treatment (day 3).

Isolation of MRSA bacteria from serum/plasma of infected mice

To recover bacteria from MRSA-infected mice for RNA and protein analyses by RT-PCR and western blots, blood was drawn from ten to twenty mice pooled in each group. For one group, a total of 3–5 mL serum/plasma was harvested, with 300 μL from each mouse. MRSA bacteria were purified by differential centrifugation and filtration, based on size differences between MRSA and blood cells. Briefly, serum/plasma was collected, and cleared by centrifugation at 500 ×g for 5 min, followed by 1,000 ×g. The supernatant was then filtered through a 5 μm filter to remove blood cell residuals. After centrifuging the filtrate at 6,000 g for 10 min, the pellet was treated with 0.1% Triton X-100, washed and resuspended in 50 μL PBS. As there were 10,000 CFUs/μL serum obtained in average (data from Figure 4E, estimated by performing agar culture), the final recovery of bacteria CFUs was ~5×10^7. The sample was then subjected to Dynamic Light Scattering (DLS) analysis to examine possible exosome contamination.

Once the purity of MRSA isolation was confirmed, they were subjected to RNA and protein extractions, for exosomal components examination. As a control, *in vitro* cultured MRSA was mixed with un-infected blood and subjected to the same procedure as *in vivo* MRSA isolated from plasma of infected mice.

Construction and characterization of the siMecA circuit

The siMecA circuit was constructed by GenePharma (Shanghai, China). The successful expression and loading of the desired siMecA guide strand into exosomes—derived from Hepa 1–6 cells transfected with the siMecA circuit—was verified by quantitative RT-PCR analysis (Figure S11).

Calculation of sRNA content in bacteria and medium

E. coli was incubated with exosomes at a final concentration of 200 μg/mL for 6 h. siAda delivered into *E. coli* was quantified by qRT-PCR, which was 9.36 fmol/10^8 *E coli* cell, calculated to be [$9.36 \times 10^{-15} \times 6.022 \times 10^{23}/10^8$ =]56 copies/cell (Figure 1A).

MRSA was incubated with exosomes at a final concentration of 200 μg/mL for 6 h. siMecA delivered into MRSA was quantified by qRT-PCR, which was 17.5 fmol/10^8 bacterial cell, calculated to be [$17.5 \times 10^{-15} \times 6.022 \times 10^{23}/10^8$ =]105 copies/cell (Figure 3A).

The siAda content was 0.3 fmol/μg exosomes, correspondingly 200 μg/mL of exosomes refers to siAda at a concentration of [$200 \times 0.3 \times 10^{-15}/10^{-3}$ =] 0.06 nM. Free siAda at the same concentration was used for incubation in Figure 1A. Lipo-siAda: we incubated 100 fmol siAda with 0.5μL of Lipofectamine 2000 (Invitrogen) for 15 min at r.t. to obtain Lipo-siAda, and its concentration for co-culture with *E. coli* was 100 fmol/mL = 0.1 nM.

The siAda content in the supernatant was 0.01 pmol/mL (medium) = 0.01 nM after 6 h of culture, whereas the content in the pellet was 5.95 fmol/10μl (bacterial volume) = 0.6 nM (Figure S1E).

QUANTIFICATION AND STATISTICAL ANALYSIS

All statistical tests were performed using GraphPad Prism v9. Data are expressed as the mean ± standard error of mean (SEM) or the mean ± standard deviation (SD). Student's t-tests (two-tailed) were used to compare two datasets. One-way ANOVA was used for experiments consisting of multiple groups, and two-way ANOVA for experiments involving two independent variables. The log rank test was used for survival analysis. The non-parametric Mann-Whitney test (two-tailed) was used to compare two groups of observations. Specific tests are mentioned in individual figure legends. The value of *n* represents biological replicates. *p* value of <0.05 was regarded as significant.